Evaluation of Transient Measurement Methods in Gas-Insulated Transmission Lines

August 1983

NBSIR 83-2753

EVALUATION OF TRANSIENT MEASUREMENT METHODS IN GAS-INSULATED TRANSMISSION LINES

Ronald H. McKnight and Howard K. Schoenwetter

U.S. DEPARTMENT OF COMMERCE
National Bureau of Standards
National Engineering Laboratory
Center for Electronics and Electrical Engineering
Electrosystems Division
Washington, DC 20234

August 1983

U.S. DEPARTMENT OF COMMERCE, Malcolm Baldrige, *Secretary*

NATIONAL BUREAU OF STANDARDS, Ernest Ambler, *Director*

TABLE OF CONTENTS

LIST OF FIGURES

LIST OF FIGURES (cont.)

Page

LIST OF TABLES

EVALUATION OF TRANSIENT MEASUREMENT METHODS
IN GAS-INSULATED TRANSMISSION LINES

Ronald H. McKnight and Howard K. Schoenwetter

Abstract

Capacitive sensors suitable for measuring transients in gas-insulated transmission lines have been studied in the laboratory. Measurements of the step response of three different sensors were made with a test line using both low voltage (200 V) and high voltage (10 kV) signals. Sensor designs were based on those used in pulse power measurements. The use of active electronics at the sensor output in the form of fast buffer amplifiers or commercial FET input probes was investigated as a means of extending low frequency cutoff. Lumped parameter models were used to provide theoretical analysis of experimental results.

Key words: capacitor sensors; gas-insulated equipment; high voltage; transient measurements; transmission lines.

1. INTRODUCTION

The use of gas insulated systems (GIS) is steadily increasing throughout the world. A recent workshop [1] dealt with gas insulated substations from the user standpoint while a useful bibliography of gas insulated substations [2] has been prepared by an IEEE working group. One characteristic of GIS is the production of significant overvoltages during various switching operations [3-5]. These switching operations can also result in a transient rise in the external sheath potential of the equipment [6]. Suitable measuring systems must be used to determine the transient conditions existing on GIS during switching operations. This is because of the fast breakdown process associated with the pressurized SF_6 gas dielectric used in gas systems. Rise times of breakdown in SF_6 may be subnanosecond under certain conditions [7], but are more typically 5-10 ns for restrikes during disconnect operations [8]. Electrically, GIS may be considered as reasonably complex transmission lines, with various surge impedances and terminations. As a result, fast transients propagate freely throughout the system with little or no attenuation of high frequencies. Both experimental observation and modeling using computer codes for transient analysis have been used to improve understanding of overvoltage production in GIS. Examples of such research may be found in the literature [3,5].

Severe requirements are placed on instrumentation to be used in investigations of transients in (and on) GIS. If information about the initial transient is required, the system must have nanosecond time response. In [3], waveforms are shown which contain both MHz and kHz components. As will be discussed later, the bandwidth of the system may be required to extend down to 60 Hz to facilitate on-site calibration. A significant transient rise in the potential of the sheath may be encountered, which can result in unacceptable noise levels and may damage equipment under severe conditions.

The purpose of the effort reported here was to investigate different configurations of capacitor sensors which could be used to make measurements of transients in gas insulated systems. A facility was developed to be used in investigations of the transient response of capacitor sensors of various configurations, including near full-scale sensors of the type installed in the Bonneville Power Administration (BPA) equipment. In addition to experimental work, calculations were made using circuit analysis codes of lumped parameter equivalent circuits to allow a comparison of experiment and theory. These and other aspects of the effort are described in detail in the following sections.

2. EXPERIMENTAL APPROACH

In order to evaluate the performance of capacitive sensors, a suitable signal source must be provided. Ideally, the step response of the sensor should be determined since the maximum information about the sensor can be determined from this type of measurement. In principle, the response of the sensor to an arbitrary waveform can be determined if the step response is known [9]. Because the dividers considered here have no discrete high

2

side capacitance, signals cannot be directly applied to the divider. Any system devised to generate a signal will have electrical characteristics of its own, which must be known if the divider response is to be determined. The use of a gas insulated transmission line for these investigations seems ideal. The impedance characteristics of a complex line can be determined using reflectometry techniques and the propagation of transients on a line can be modeled. Step signals can be readily generated on a transmission line. One means of generating a step signal is to use a cable pulser with a mercury-wetted relay. Such a pulser is shown schematically in figure 1. The charge line is charged to V_o, then discharged into the gas transmission line, figure 2. If the line impedances are equal and the gas line is terminated, in the characteristic impedance, a step will propagate down the line with magnitude $V_o/2$ and step length equal to twice the electrical length of the charge cable. Because of limitations on the relay, maximum signals are limited to a few hundred volts. This signal level is satisfactory for some types of testing but provides inadequate signal levels if the divider ratios are 10^5 or larger. In principle, the pulse can be made as long as desired, but a practical limit is a few microseconds, due to losses in the charge cable.

A second method for generating a step is to charge the gas line itself to some voltage and then discharge the line into its characteristic impedance. Since the line can be charged to higher voltage and discharged through a spark gap, much larger signals can be generated in this way than with the pulser. However, pulse lengths are limited unless a cable extension can be provided to increase the effective electrical length of the gas line. In figure 3 is shown a pressurized gas switch along with a large diameter extension. The gas switch was used to provide high voltage ($\sim$ 10 kV) pulses as described above, while the extension was used to investigate full-scale sensors of the type found in BPA equipment.

Although the coaxial cables, gas line, and extension are all designed for a nominal 50 Ω impedance, there are obvious geometric mismatches at the input and the line-extension transition. Also, the switch assembly does not have a constant impedance. Although smoother transitions can be made by using tapered lines or appropriate designed stepped sections, no attempts were made to improve the impedance uniformity of the test facility during the work reported here. The effects of these mismatches resulted in reflections and a waveform which deviated from a smooth step after approximately 18 ns. These phenomena are discussed in more detail in following sections.

A transient digitizer and associated control unit were used for data acquisition and manipulation. The digitizer unit has a maximum effective sampling rate of 100 GHz and was used with a vertical amplifier with a 500 MHz bandwidth and an effective rise time of 0.8 ns. A 100 MHz storage scope with an effective rise time of 3.5 ns was also used for some measurements. The digitizer-controller combination provides hard data storage as well as the capability for extensive data manipulation and plotting.

Examples of the output waveform from the cable pulser are shown in figures 4-6. These data were acquired by using a low charging voltage and discharging the pulser into the same signal cable used in the divider measurements. This signal cable was 11.6 m of RG214/u and was used in all measurements reported here unless noted. Although mercury-wetted

3
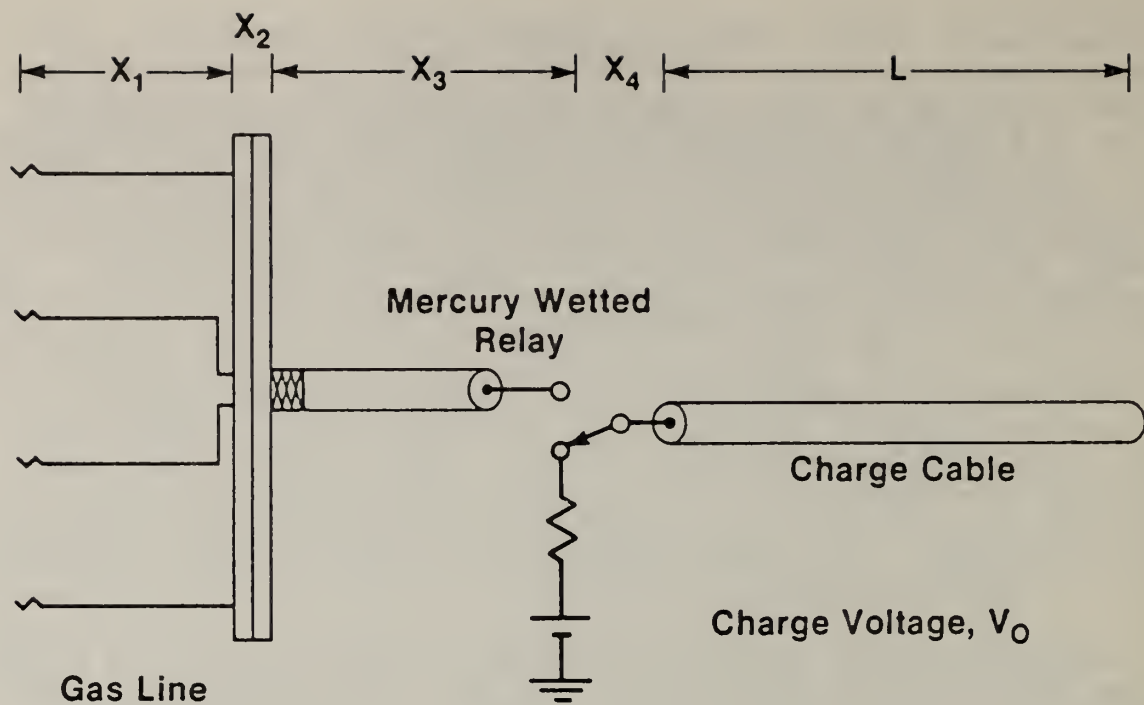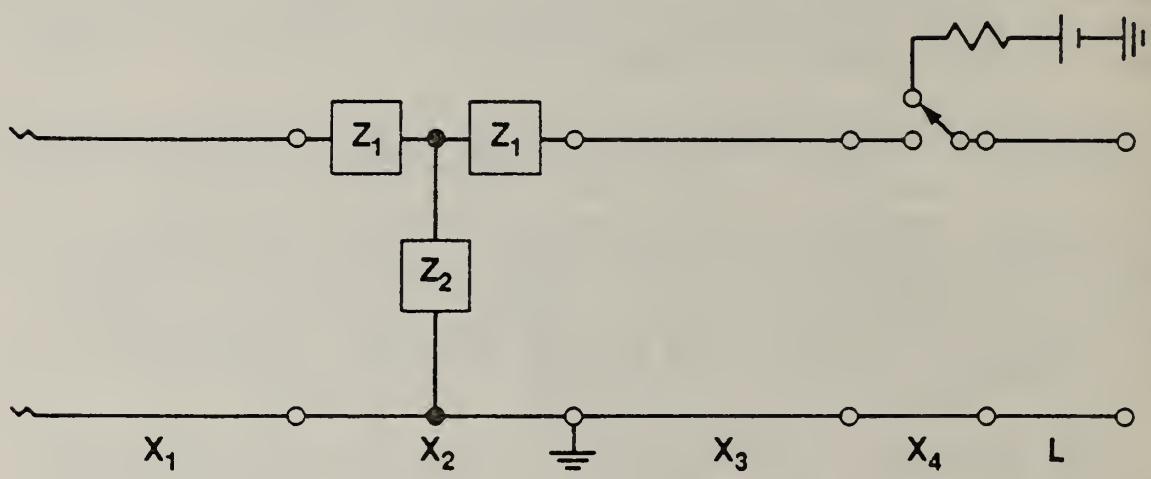
Figure 1.   (a) Mercury-wetted relay cable pulser.   Driver circuitry
             is not shown.

            (b) Transmission line equivalent circuit.   Impedances represent
                discontinuities at input to test line.

4
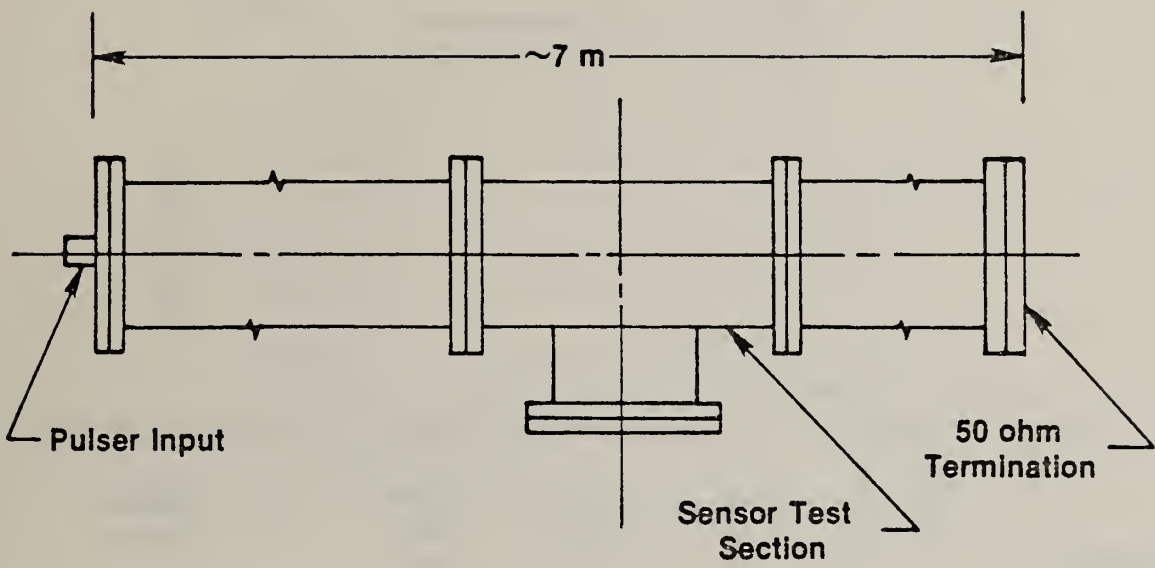
Figure 2.   Coaxial test line for transient measurements.
Line diameter is 0.15 m.

5
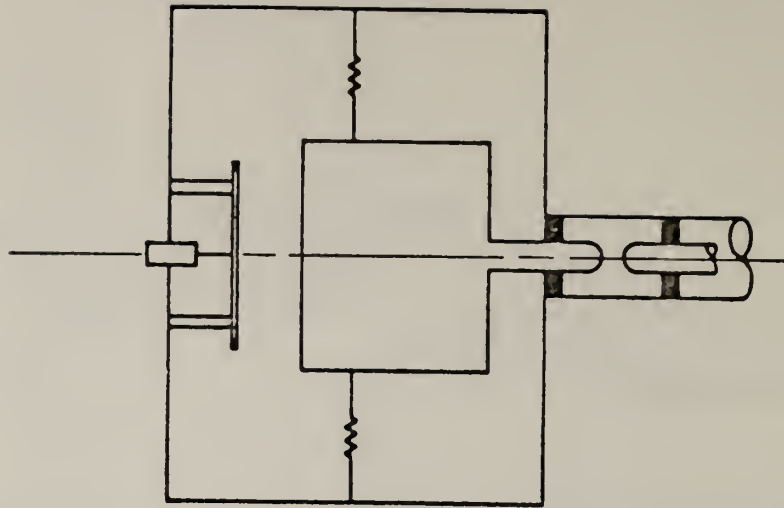
(a)
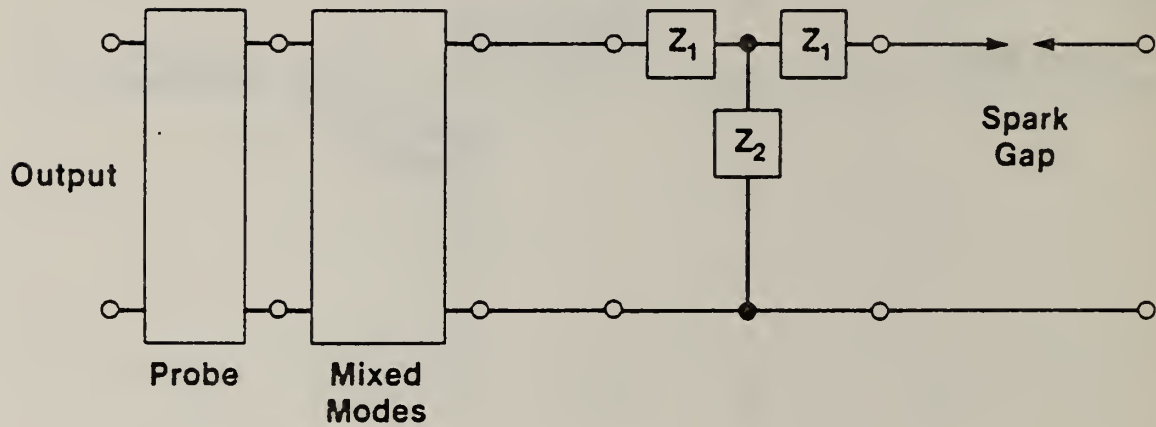
(b)

Figure 3. (a) Schematic view of test line extension and high voltage
          spark gap. Extension diameter is ~1 m. Line is
          terminated with resistor spider (50 Ω).

          (b) Transmission line equivalent circuit, showing impedance
          mismatch at geometric transition. Propagation involves
          mixed modes in extension section.

6
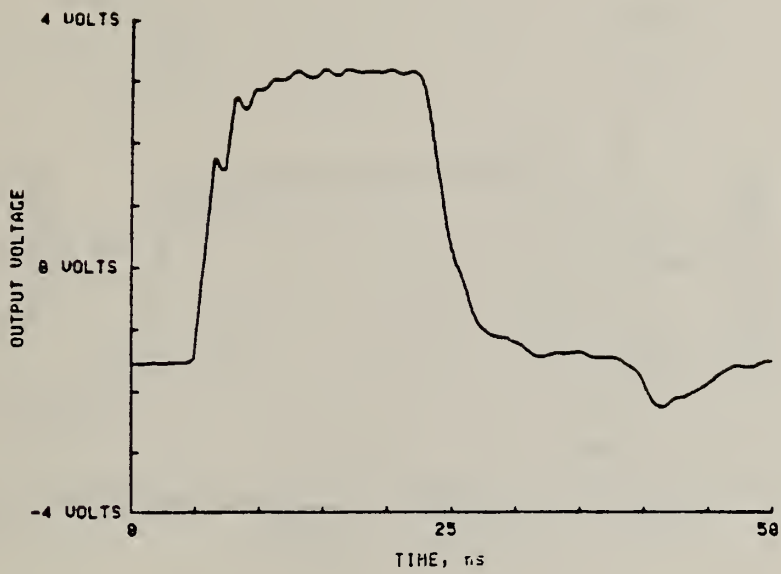
Figure 4.   Direct pulser output for short charge cable.   Output
voltage when driving test line would be ~200 V.
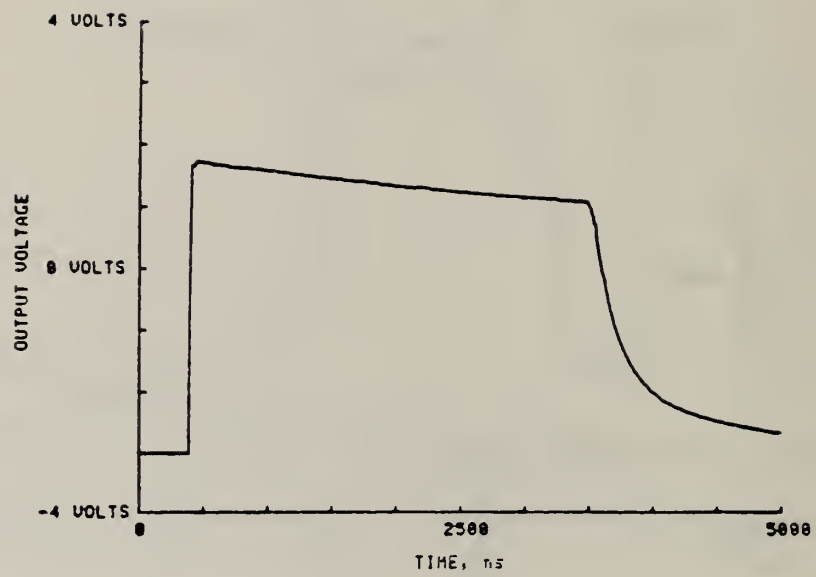
Figure 5.   Direct pulser output for 305 m of RG58/U. Droop is
due to cable loss.
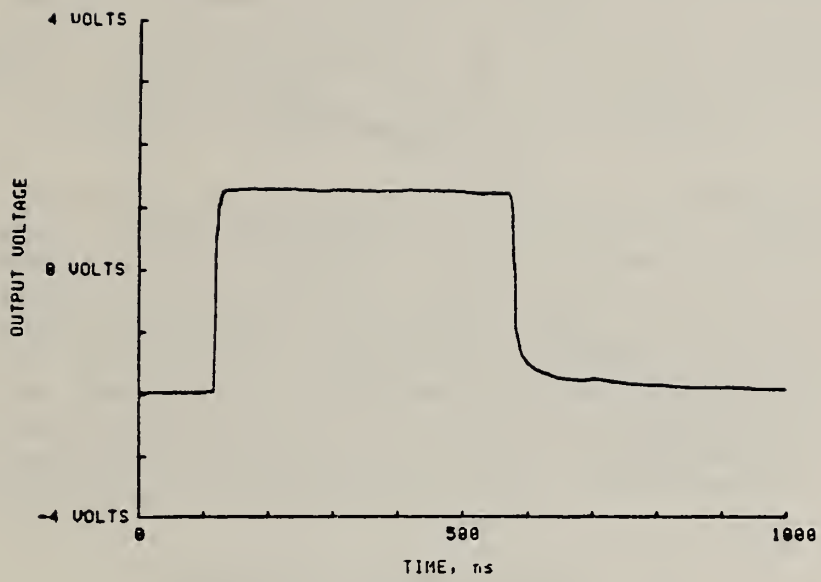
Figure 6.   Direct pulser output for 46 m of RG214/U. This cable
was used for most measurements reported here.

relays can produce sub-nanosecond rise time pulses, the pulser configuration used here had a rise time of approximately 2 ns as shown. Relays are not available with 50 Ω geometry, so stray impedances in the pulser assembly are probably responsible for the structure on the leading edge. The droop in the signal for the long cable is due to losses in the cable. Although a faster rise time would be desirable, the signals are adequate for much of the investigation of the capacitive sensors reported here. In actual operation, the charge voltages are several hundred volts, but a direct measurement of the pulser output at these voltages is not possible because of equipment voltage limitations, i.e., the lack of a suitable high speed, high voltage attenuator. This is not a serious limitation to the work presented here.

The high voltage switch was operated at various pressures of dry air and breakdown characteristics determined for different gap spacings. A gap spacing of 1.32 mm and a pressure of 0.219 megapascals (30 psi) allowed a charging voltage of 20 kV. Figure 7 shows the output of a disk configuration divider (discussed later) for a 20 kV charging voltage. This charging voltage corresponds to a 10 kV pulse on the line. The rise time is approximately 2 ns, which is comparable to that achieved with the pulser.

The oscillations in the divider output are not associated with the divider, but appear to be due to the impedance mismatches in the line discussed earlier. It was also found during the high voltage tests that there was a transient ground potential increase. This increase was estimated to be less than 200 V by using a capacitor divider located external to the test line. A careful series of measurements indicated that reliable data could be taken using the digitizer and control unit without any special shielding or noise suppression measures. During the measurements reported here, the gas transmission line was grounded at several points to a local ground line. The laboratory floor did not contain a well-defined ground plane.

2.1 Transient Sheath Potentials

In addition to the transients that are generated inside GIS during switch operations, it is possible that significant potentials appear on the ground sheath [6]. These potentials can cause difficulties in the measurement process in the field. The possibility of similar transients exists in the laboratory during operation of the test line in the high voltage mode. Such transients were indeed observed, but as noted above, the transient were not sufficiently large to present any measurement difficulties.

Preliminary calculations have been made to model the laboratory gas line during different switching experiments. These calculations, along with experimental results, are useful in determining possible deleterious effects on measurements during switching opertions and in aiding investigations of means of accurately measuring sheath transient potentials.

The transmission line used in the calculations is illustrated in figure 8. Although only one ground strap is indicated in figure 8, any configuration of different strap locations is allowable. The equivalent circuit for the model is shown in figure 9.

10
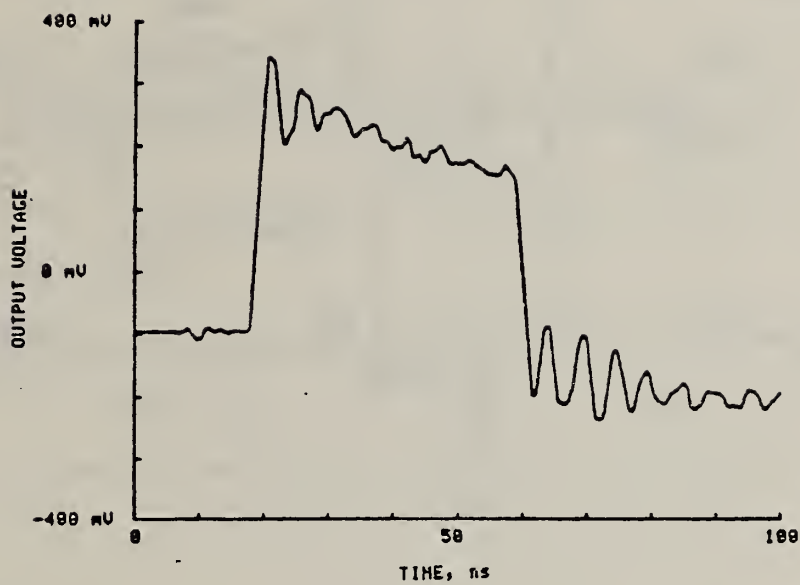
Figure 7. High voltage signal produced when line (fig. 2) is charged to 20 KV and discharged through switch into line extension (fig. 3). Sensor was plug sensor (fig. 13).
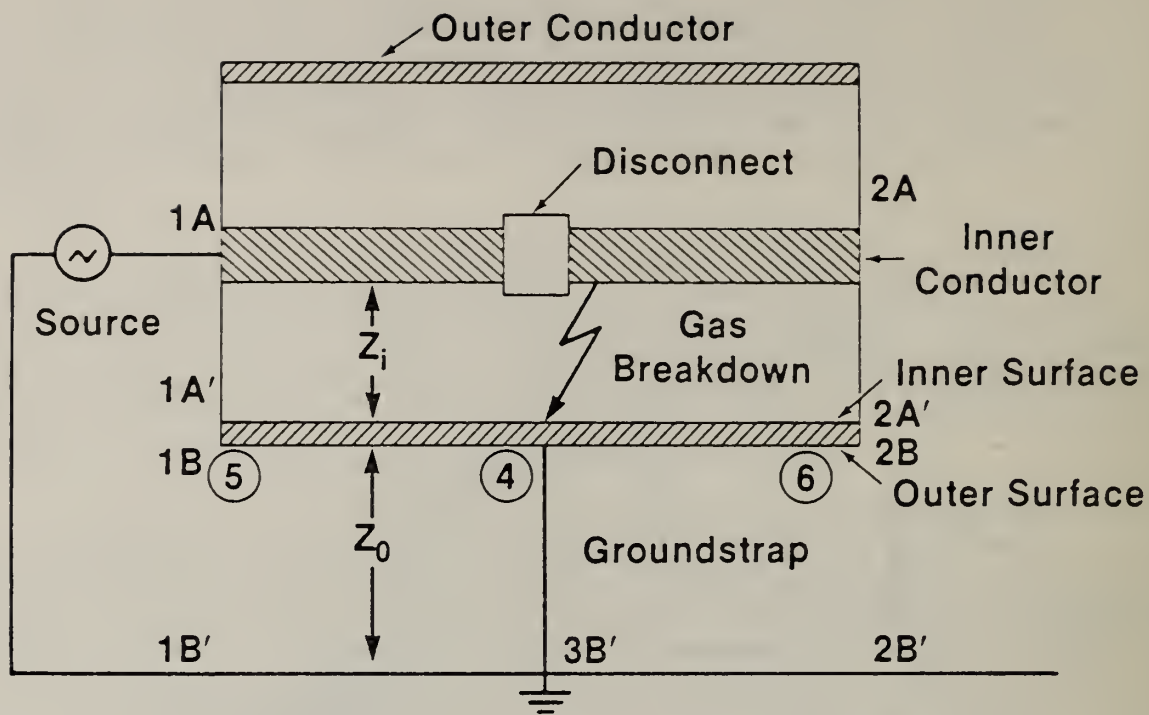
Figure 8. Model for short gas-insulated transmission line, which may have a breakdown to the outer sheath, or a disconnect switching operation in the center conductor.
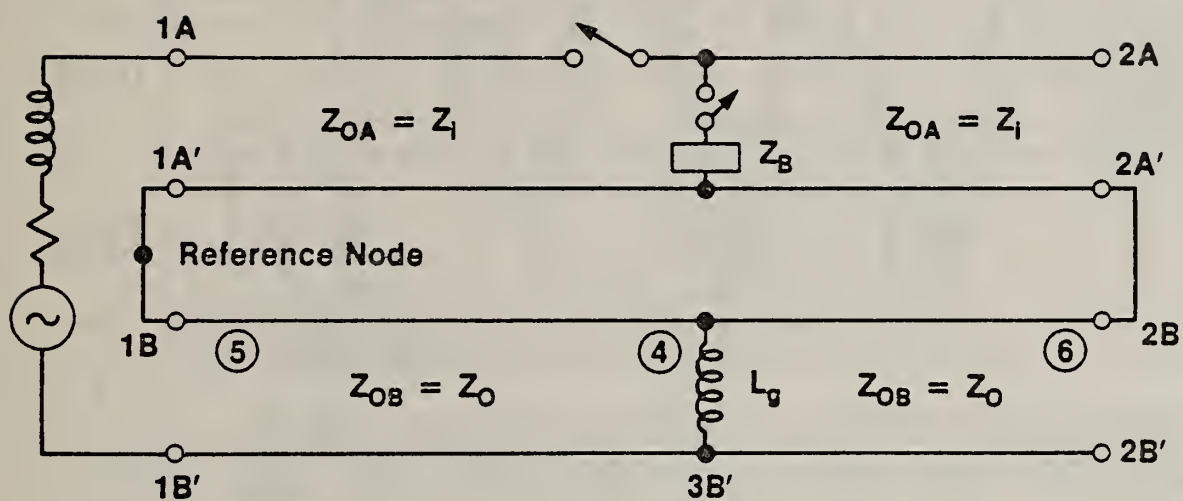
Figure 9. Equivalent circuit for model shown in figure 8. Nodes are as indicated in figure 8. Transient voltages resulting from disconnect operations were calculated for points 4, 5 and 6 (see figs. 10 and 11).

2.2 Model for Short Gas-Insulated Conductors

The object of the model is to represent a short gas-insulated conductor during internal switching or gas breakdown inside the pipe. The model is digitally simulated by the Electromagnetic Transients Program (EMTP) which is used as follows. A circuit composed of distributed lines, lumped impedances, switches, and sources is specified using the circuit nodes for identification. The EMTP sets up the initial conditions (trapped charge, etc.), and time-integrates the nodal equations. Any node potential or branch current can be listed and/or plotted. The details of model elements used in the calculation are discussed below. The conductor and pipe with impedances Z_i and Z_0, respectively, are considered as two separate transmission lines. A coaxial transmission line consisting of the conductor and the inner pipe surface of surge impedance $Z_i = 60 \ln (r_i/r_0)$ where r_i = pipe inner radius and r_0 = conductor radius is in series with a transmission line consisting of a cylindrical conductor over the ground plane of surge impedance, $Z_0 = 60 \ln (2h/r_z)$. Here h is the height of the pipe center above the ground while r_z is the pipe outer radius.

The source (V) is represented by a 60 Hz sinusoidal voltage and its associated impedance which, in this case, is assumed to be inductive. The groundstrap (Lg) is modeled by a lumped inductance of 0.9 μH [6]. The internal switch (S_1) which simulates a disconnect is modeled by a switch which at its position on the conductor closes at time 0^+. Trapped charge is allowed for. Flashover to the sheath can also be modeled. In this case S_2 and Z_B are modeled by a switch which also closes at time 0. Two examples of calculations made using EMTP are shown in figures 10 and 11.

Both figures represent a disconnect calculation. The only change in the two calculations is the value of the source inductance as indicated in the captions. The order-of-magnitude difference in voltages appearing on the sheath is indicative of the importance of source impedance in this calculation. Voltages are shown at three different locations, and the complex waveforms generated are indicated.

Measurements were made in the laboratory for an experimental configuration where a gap was placed in the inner conductor of the gas line, but the outer conductor remained continuous. The gap broke the coaxial line into two segments of (2/3)L and (1/3)L, where L is the line length. The longer segment was then charged so that an overvoltage was applied to the gap. Measurements were made of the signal appearing on the outside sheath using both the plug capacitive divider described below and a small fast resistor divider. These measurements were made for different charging resistors placed between the gas line and the high voltage supply. As the charging resistor was varied from 5 MΩ to zero, the observed overvoltage increased by approximately a factor of 10. These measurements were made with a single ground strap on the line as in figure 8. However, because of the presence of supports for the line and a lack of knowledge of the actual impedance of the high voltage source, it is not expected that there would be quantitative agreement between theory and experiment. An example of the signals observed is shown in figure 12. These were taken at a location corresponding to location 6 in figure 8 using the plug capacitive sensor, located beneath the transmission line at a distance of approximately 10 cm.
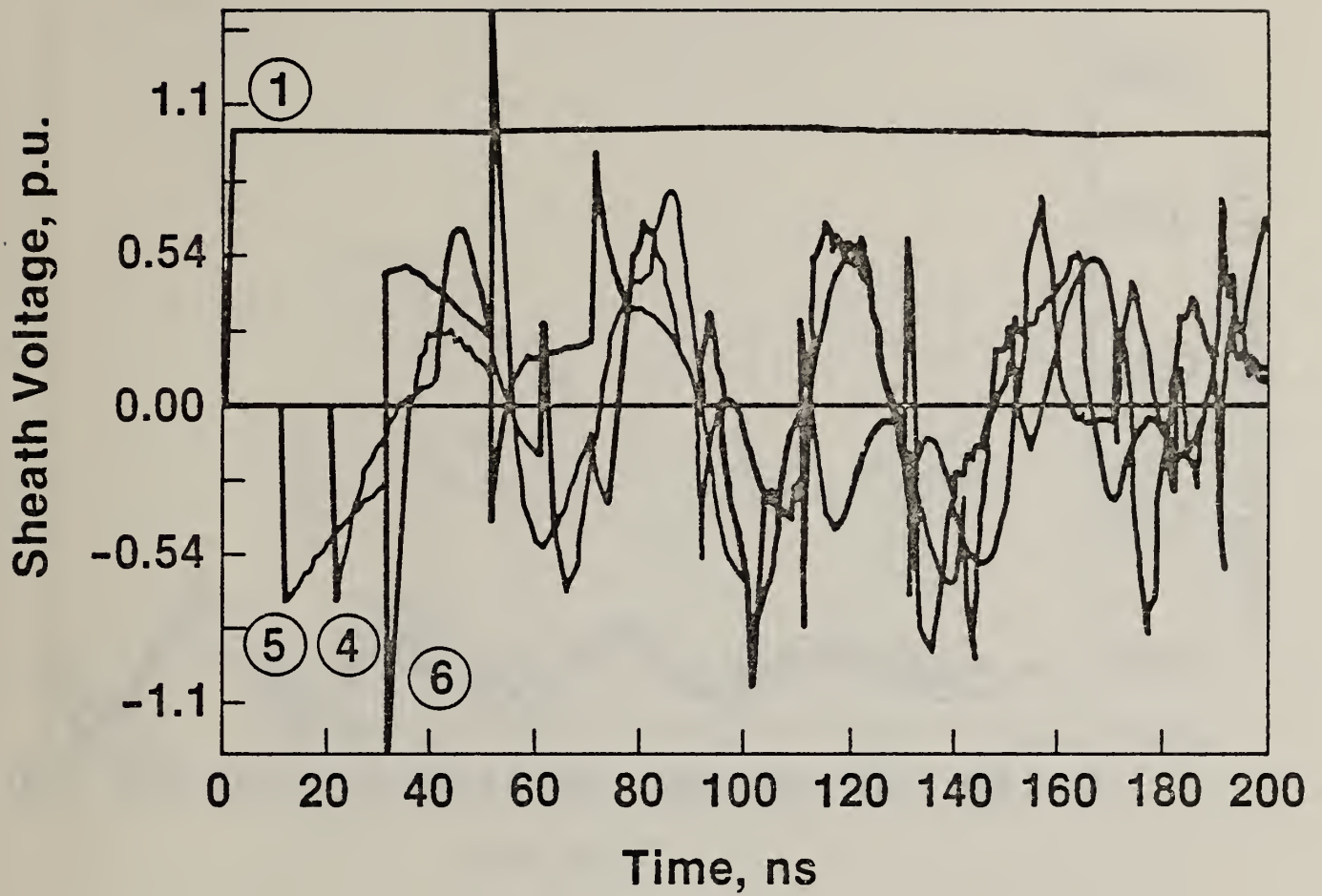
Figure 10. Calculated waveforms for locations 4, 5, and 6 in
figure 8. Source inductance was 1.6 nH. The
assumed source function was a 1 p.u. step.
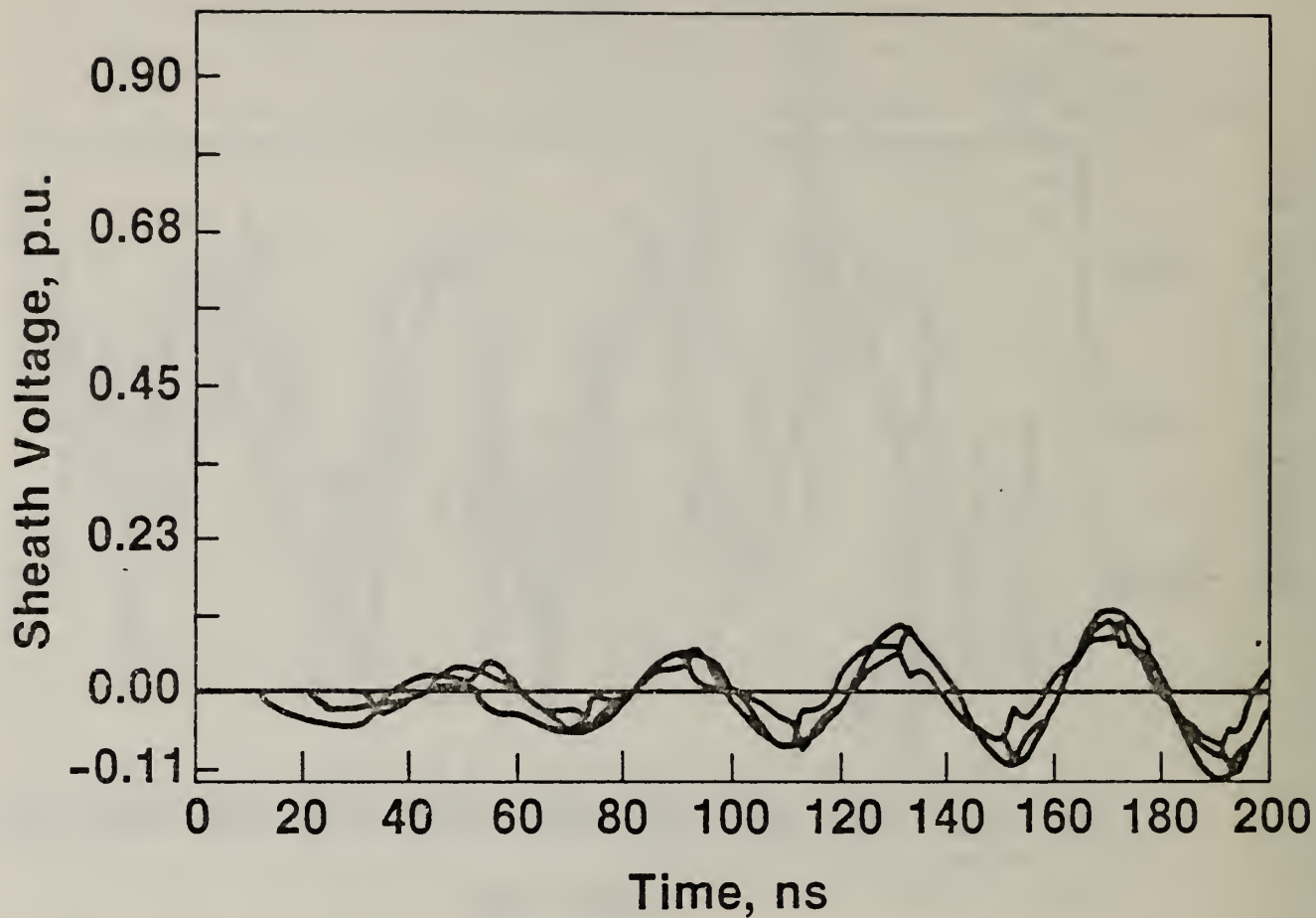
Figure 11.   Calculations for the line as indicated in figure 10, except for a larger source inductance (0.16 mH). Note significant difference in sheath voltage magnitude between calculations shown in figures 10 and 11.
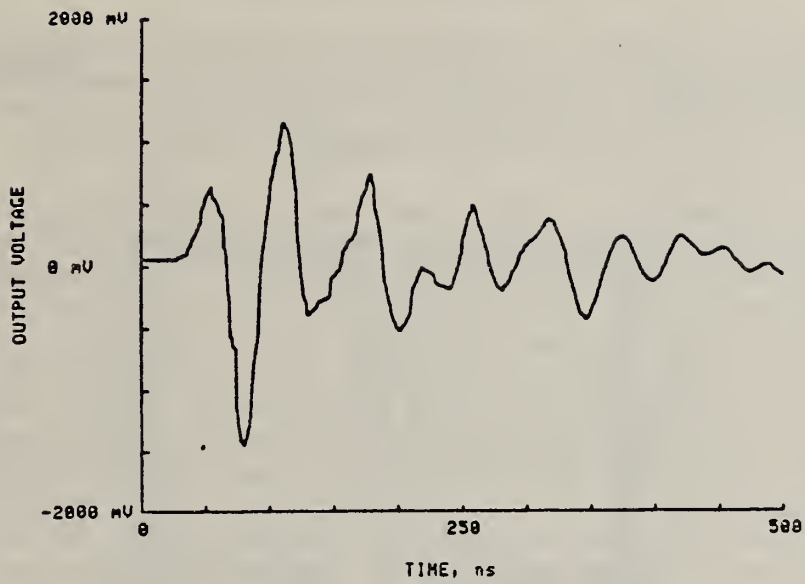
Figure 12. Sheath signal measured with plug capacitive sensor located at
location 6, with no charging resistance between high voltage
supply and transmission line (see text).

17

These measurements indicated that for a charging resistance of 5 MΩ and a charging voltage of 10 kV, transient signals on the sheath were less than 200 V. A series of experiments were done which indicated that data could be taken using the digitizer and controls even when the line was operated in a high voltage mode, when the extension was in place.

The results and calculations for sheath potential rise discussed above are preliminary and do not represent an extensive effort. They are a useful introduction to the use of theory and experiment to investigate transient phenomena generated on the sheath of a gas transmission line in the laboratory.

3. SENSOR CONSIDERATIONS

Although GIS are usually equipped with precision voltage and current measuring devices, these are not useful for transient measurements because of restricted bandwidth. An example of instrumentation designed specifically for GIS, but not for transient measurements, is found in [10].

Conventional impulse dividers have been used in certain measurements [3,6], but cannot be used to detect transient voltages internal to the gas equipment. They are also limited in high frequency response. Fast compensated resistor dividers have been used in pulse power systems [11], but in this case there is no steady-state voltage and low impedances can be tolerated. Simple capacitor sensors have been used in short pulse high voltage applications for many years [12,13] and appear to be ideally suited, with suitable modifications, for use in GIS. High voltage capacitor dividers for freestanding use have been described in the literature [14] and in measurement textbooks [15,16]. One configuration of a divider suitable for use in gas insulated equipment is shown in figure 13, while a simple equivalent circuit is shown in figure 14. The advantages and disadvantages of this (and similar) dividers may be seen from figure 14 and the calculated step response,

$$V(t) = \left(\frac{C_1}{C_1 + C_2}\right) \left(\frac{R_2}{R_1 + R_2}\right) \exp(-t/\tau) \quad , \tag{1}$$

where the time constant τ of the circuit is given by

$$\tau = (C_1 + C_2)(R_1 + R_2) \quad . \tag{2}$$

It is generally recognized that these capacitor dividers which are integral to the system are capable of subnanosecond response and this has been shown in other applications [7,8]. The bandwidth problem lies in the low frequency response. If the transmission line is terminated in its characteristic impedance to avoid reflections at the measuring device, then the practical lower cutoff frequency can be high. For example, the calculated low frequency cutoff with R_1 and R_2 equal to 50 ohms is

$$f_{co} = 1/(2\pi\tau) \approx 1.5 \text{ to } 0.15 \text{ MHz} \tag{3}$$

for typical C_2 values of 1 to 10 nF.

This analysis is based on the simple treatment of the circuit as a high pass filter. This cutoff situation can be improved by increasing R_2. In

18
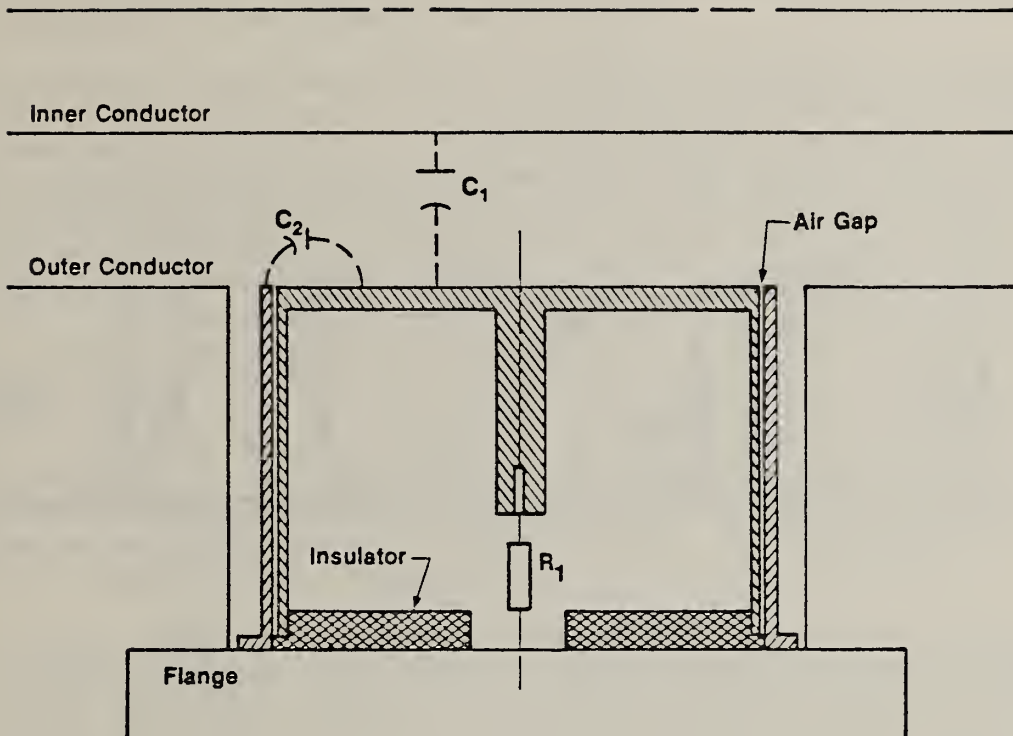
Figure 13. Plug sensor inserted in "T" section of test line. Plug diameter is 0.12 m.
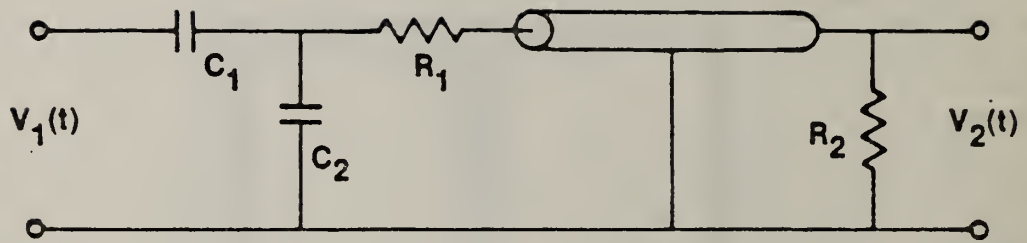
Figure 14. Simplified equivalent circuit for capacitor divider.

a later section, consideration is given to the use of active electronic circuitry in the low divider output side to extend the cutoff frequency to below 60Hz. A second problem is associated with the fact that C_1 is not a discrete component, but represents the coupling capacitance between the sensor and the high voltage electrode. This means that the divider cannot be evaluated as a stand-alone unit. The step response of the divider and its attendant measuring system can be studied in the laboratory, but not with the identical C_1 that exists in the actual system. As a result, the final calibration of the divider must use methods suitable for an in-place calibration. This is a non-trivial problem. With regard to calibration, it should be made clear that the achievable accuracies associated with these measurements will not be comparable to those of potential transformers, although they should be adequate for anticipated requirements.

Other special requirements may be placed on the design of a suitable capacitor divider. Voltage limitations on low side components may place requirements on the C_1/C_2 ratio. If active components and optical links are to be used [17], then overall system integration must be considered. Physical constraints may dictate the geometry of the divider. Despite all these special conditions, it is possible to learn a significant amount by doing laboratory investigations of model or full-scale sensors.

A series of measurements was made using three different divider configurations. One of these, the "plug" sensor, is shown in figure 13. In the plug sensor, there is almost complete shielding except for the portion of the center element exposed to the high voltage electrode. The low side capacitor C_2 is an air-dielectric coaxial capacitor. Three-terminal capacitor measurements were made of C_1 and C_2 for this sensor installed in the tee of the transmission line (see fig. 2). The values obtained were 1.012 pF and 1.107 nF, respectively.

A second configuration is shown in figure 15. Here C_2 is a folded parallel plate capacitor. The dielectric was 10 mm thick polycarbonate. This material was chosen because of availability at the time of divider construction. The ratio of the divider can be changed by varying the size of the opening in the top plate, which affects both C_1 and C_2. Other dielectric materials may be used as well. The thickness of the brass plates making up the unit was 0.79 mm. This is significantly greater than the 1 GHz skin depth.

The third divider (the BPA divider) is shown schematically in figure 16. The sensor, which is 0.4 m (16 in) in diameter, was intended to simulate the disk sensors installed in BPA equipment. The spacing above the sheath was chosen to be approximately that for the actual sensor. A nylon feedthrough carried the signal from the disk through the enclosure wall to a small shielded box in which C_2 was mounted.

Two different configurations for C_2 were used in these investigations. The purpose of changing C_2 was to vary the inductance associated with the low side capacitance. To produce a minimum inductance configuration, 10, 0.01 μF, miniature ceramic capacitors were soldered between two brass plates. The capacitors used were designed for microwave circuitry.
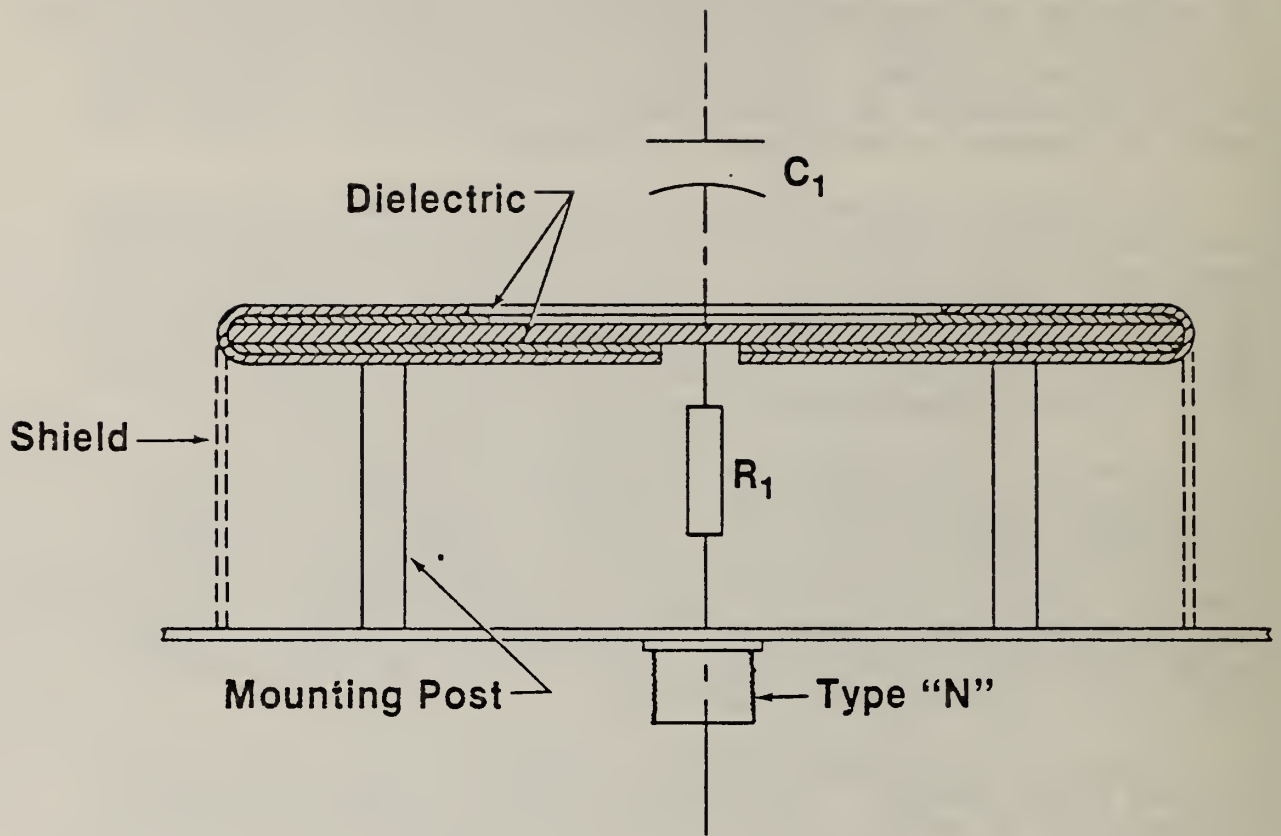
Figure 15. Cross section of disk sensor. Thickness of dielectric is exaggerated for clarity. Standoff mounting was also used. Measurements were made with and without shielding skirt.
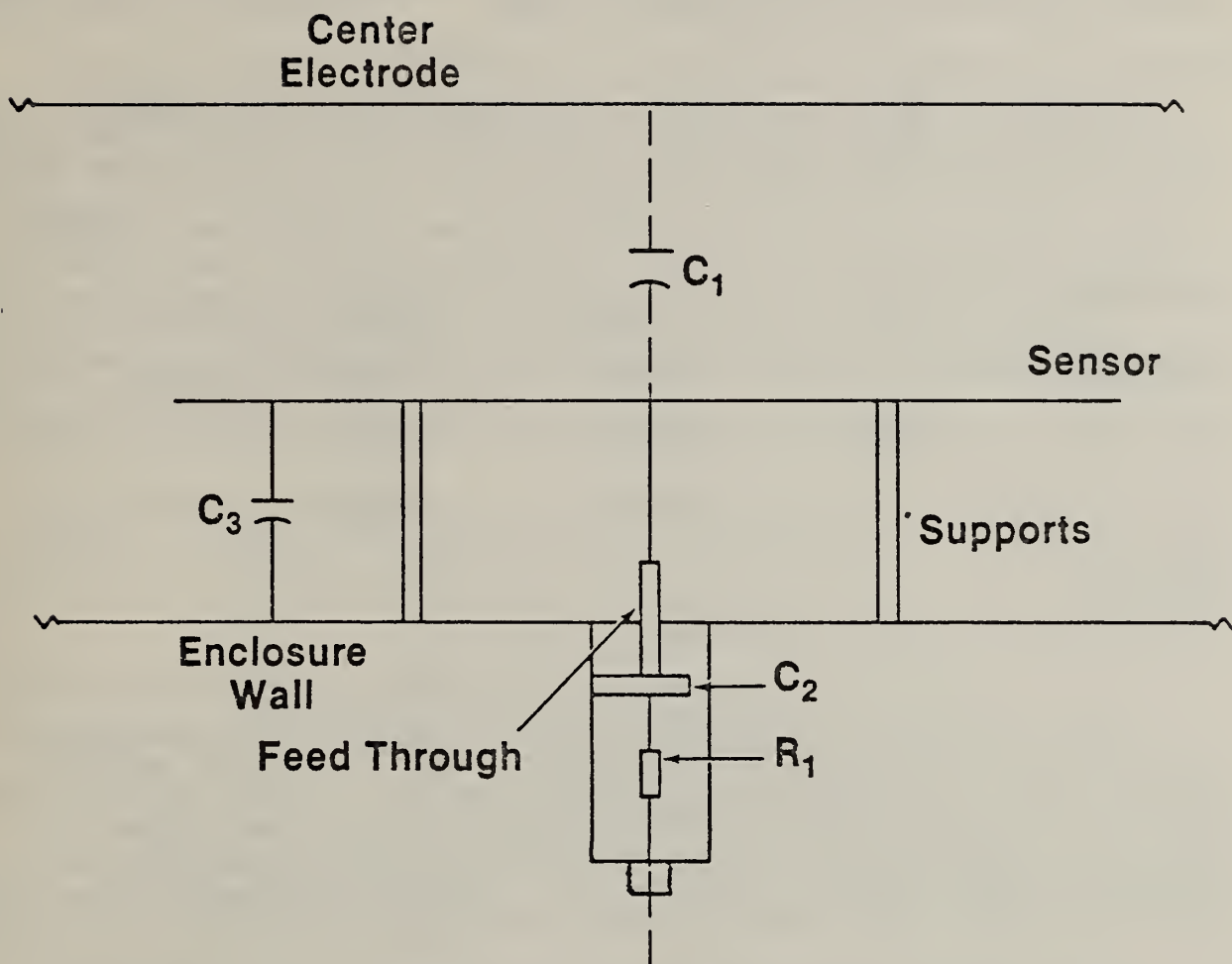
Figure 16.   Schematic of model BPA sensor.

This assembly was mounted on the feedthrough and one plate was grounded directly to the shield. A second, more inductive, low side consisted of a single 93 nF disc ceramic capacitor connected between the feedthrough and the box.

Dividers with coaxial geometry such as those described in [7,18] were not considered. This was because their installation in existing equipment requires significant disassembly, whereas the plug or disk sensors can be readily installed on existing flanges. They do represent a viable alternative to disc-type sensors for new equipment design.

Table 1. Capacitance values and calculated ratios for sensors

	C_1	C_2	Ratio[c]
PLUG SENSOR - in line	1.012pF[a]	1107pF[a]	4.57 x 10^{-4}
PLUG SENSOR - end	0.46pF[b]	1107pF[a]	2.08 x 20[-4]
DISK SENSOR - 2" spacer	0.4pF[b]	1340pF[a]	1.49 x 10^{-4}
BPA MODEL SENSOR	9.4pF[b]	96300pF[a]	4.88 x 10^{-5}

[a]measured
[b]calculated
[c]calculated for $R_1 = R_2 = 50$ Ω (see fig. 14)

The plug sensor could be mounted either in the tee of the transmission line (fig. 2) or in the end of the extension (fig. 3). The disk and BPA dividers could only be mounted at the end of the line. Table 1 summarizes the measured or calculated capacitances associated with the three dividers, and their ratios based on eq (1). The results for the three sensors will be presented as they occurred chronologically, since the development of the disk sensor was based to some extent on results obtained from the other two sensors.

A more realistic equivalent circuit for a capacitor or divider than that shown in figure 14 would be one in which various stray capacitances and inductances are included. The inductances are particularly important because of the large impedances resulting from high frequency signals. A more fundamental question concerns the validity of using lumped parameter equivalent circuits. Skin effect phenomena at high frequencies cause signal propagation along, rather than through, conductors so that a transmission line approach may be more relevant. Wave propagation on the divider itself may result in oscillations which are not predicted from the lumped parameter model. The frequency of these oscillations would be geometry dependent. This means that evaluations of various divider configurations must be made with near-full-scale configurations. Oscillations of scaled models, which are beyond the range of measuring instruments and therefore unobserved, may become dominant for full-scale devices.

The simple circuit of figure 14 cannot be expected to model adequately real capacitor dividers. A more realistic circuit is shown in figure 17. Here various stray elements have been included. Other circuits could be proposed but the salient features of the experimental results can be explained qualitatively using this model. The complicated ladder network around the low-side capacitor C_2 was not used in the present calculations but has been retained for possible future work. The capacitance to ground C_3 is an important part of the BPA sensor. It results from the location of the sensor above the ground plane. For the plug and disk sensors, this stray capacitance is negligible.

The main capacitance elements C_1, C_2, and C_3 can be measured or calculated. Resistances R_{11}, R_1, and R_2 are discrete components. Stray inductances L_8 and L_9 cannot be measured but their composite value was deduced by comparing theory and experiment. This was done by using known (calculated) values for C_1, C_2, C_3, R_1, R_2, and R_{11}, and varying L_8 until the step response ringing approximately matched the experimental value of 73 MHz. Then L_8 and L_9 were varied until both ringing frequency and divider ratio approximately matched experimental results. The goal of this exercise was to obtain an equivalent circuit which provided reasonable agreement with experimental results. Circuit values obtained in this way are given in table 2. The inductance values are small, but their effect is dramatic. The results of calculations are shown in a series of figures beginning with figure 18.

Table 2. Circuit values used in calculations for BPA model sensor[a]

C_1	-	29.4 pF
C_2	-	95 nF
C_3	-	35.2 pF
L_8[b]	-	105 nF
L_9	-	5 nF
R_1	-	50 Ω
R_2	-	50 Ω
R_{11}[c]	-	5 Ω, 50 Ω

[a]Refer to figure 17. R_8, L_4, L_5, L_7, L_{10}, C_5, C_6 were assigned negligible values.
[b]The total inductance for L_8 plus L_9 was 110 nF.
[c]The 5 Ω value was required to reproduce the observed damping, while the 50 Ω value was used to calculate the overdamped response.
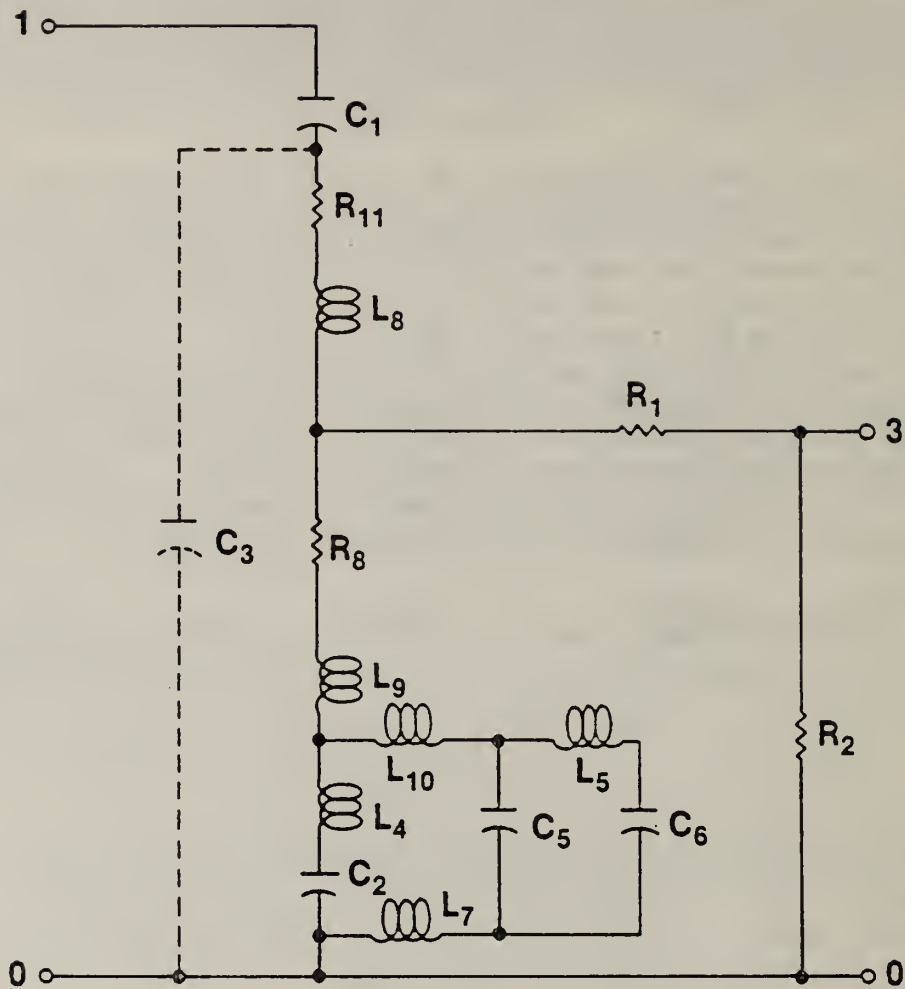
Figure 17.   Lumped parameter equivalent circuit used in theoretical calculations.   Various elements were assigned negligible values during calculations.
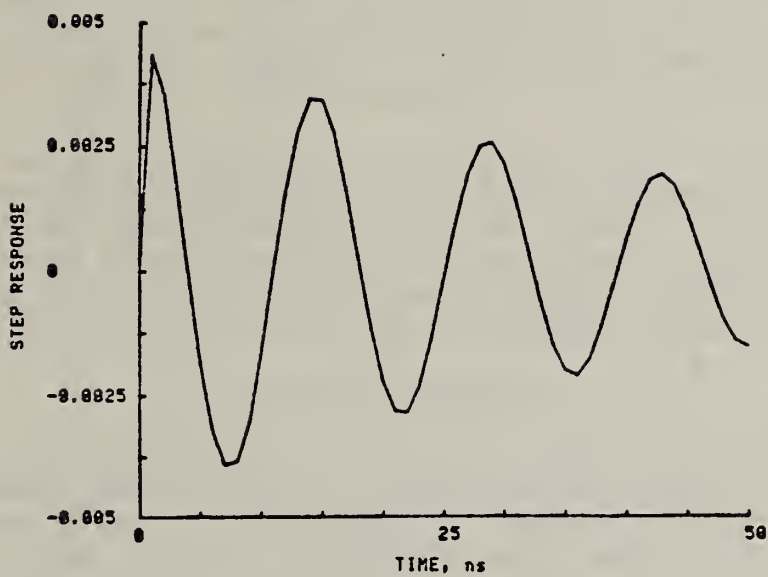
Figure 18.   Calculated step response for divider with C_1 = 9.4 pF,
C_2 = 95 μF, C_3 = 35.2 pF, R_1 = 50 Ω, L_8 = 105 nH,
and L_9 = 5 nH.   All other components were assigned
negligible values (see fig. 17 and table 2)

In figures 18 and 19, results for two different values of L_9 are shown. The ringing frequency changes are small but the amplitude of the step response changes significantly. When $R_{11} = 50$ Ω, a damped response is obtained, as is shown in figure 20. This should be compared to figure 26 below. Note that the 600 MHz signal seen in the lab (fig. 24) is not present in the step response.

From these calculations, it is clear that very small inductances in the low side cause significant deviations from capacitive response. This is not a new result and the importance of good low-side capacitor design for use in impulse dividers is discussed in the literature [14,25]. The absence of observable oscillations which can be assigned to the dividers indicates that there is very little inductance associated with either the plug or disk dividers. This is perhaps to be expected since the low sides in each case are short transmission lines. For the plug sensor, the calculated inductance per meter is 0.8 nH, which corresponds to a total L of 0.06 nH. A meaningful similar calculation for the disk cannot be readily made. Because the outputs of these low-side transmission lines are not terminated in their characteristic impedance, there could be ringing. However, because of the small dimensions involved, this ringing would be in the GHz or higher range.

Despite the list of problem areas, fast capacitive dividers have been widely used to measure pulses of short duration, particularly in pulse power systems. A recent workshop highlighted measurements of electrical quantities in pulse power systems, and several papers presented at the workshop addressed various aspects of these capacitive sensors [18-21]. Other examples of applications are found in the literature [22-24].

4. EXPERIMENTAL RESULTS

The plug sensor was chosen for use as a reference sensor because earlier reports [13,18] indicated its usefulness for short pulses, as well as the fact that it could be located both in-line and at the end of the transmission line. Figures 21(a-c) show output signals from the plug sensor for an in-line location, where the pulse on the transmission line was generated by the relay pulser and corresponds to figure 6. (In fig. 21 and others following, the same signal is shown on different time scales.) Unless noted, all experimental results are direct outputs from the sensor for a given input signal. The rise time of the signal is not significantly changed from that of the input pulse, and the time constant of the output signal is clearly evident in figure 21(c). The disturbances on the signal at approximately 18 ns after the start of the pulse appear to be due to reflections from the geometric transition at the line extension. There is no obvious oscillation or overshoot associated with the divider itself, at least within the bandwidth of the measuring system. It should be noted that the pulser output was very reproducible so that the consecutive records were nearly identical. The response of the divider to a short pulse is indicated in figure 22. In all of the records taken with this sensor, there was no indication that divider response deviated significantly from that predicted by eq (1). The observed waveforms assume a different character when the sensor is mounted at the end of the line. Data were acquired for both a flush mounting, where the face of the divider was flush with the end and for a configuration where the divider assembly was inserted into the line up to the mounting flange. A limited amount of data was acquired for the inserted configuration and, except for a change in ratio (due to the larger C_1),

28
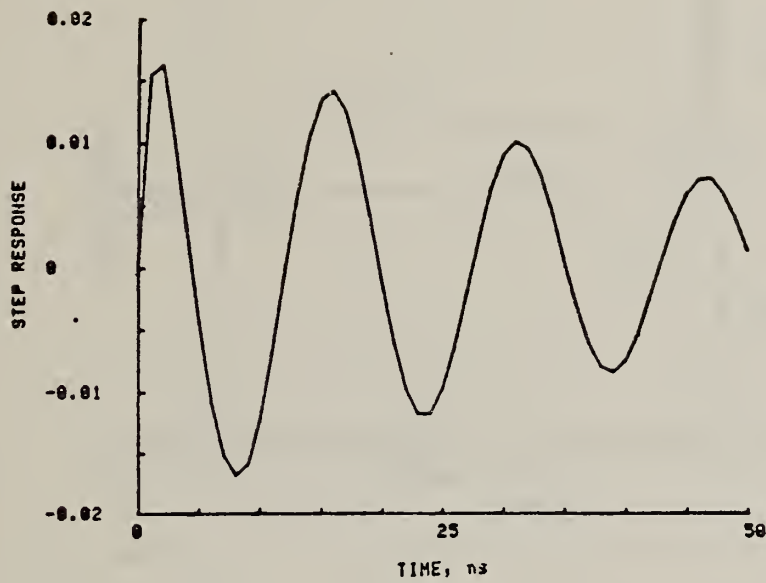
Figure 19.   Calculated step for divider with Lg increased to 25 nH.   All other component values are the same as in figure 18.
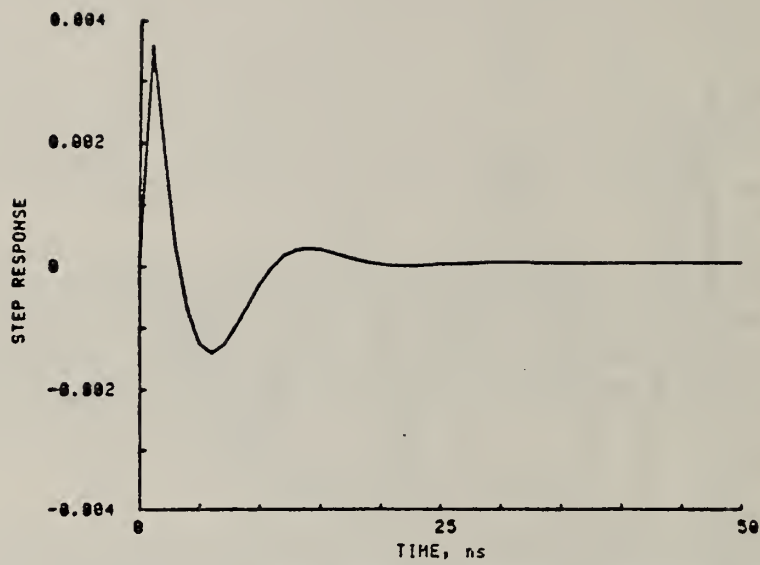
Figure 20. Calculated step response for divider with component values as in figure 18, except R11 = 50Ω.
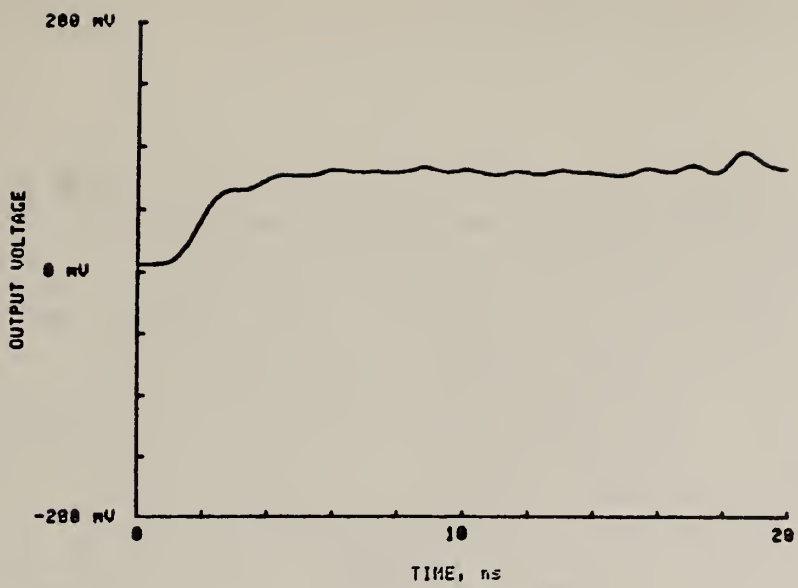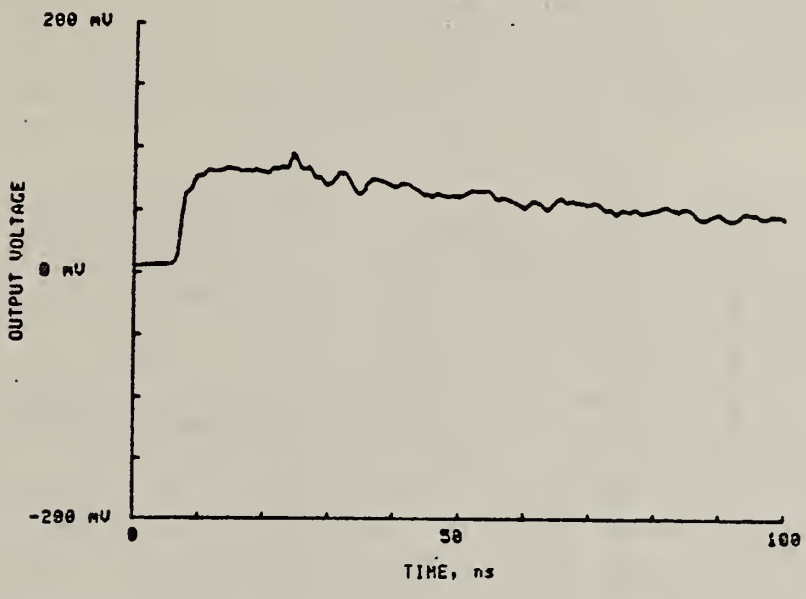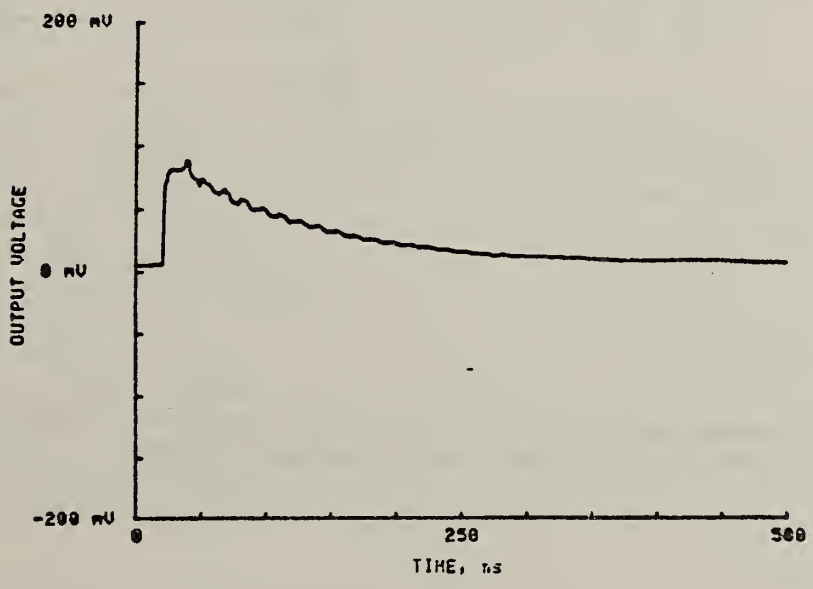
Figure 21. Output voltage from plug sensor mounted in line. Signal on line was from cable pulser (fig. 1). Charge voltage was 385 V.

31
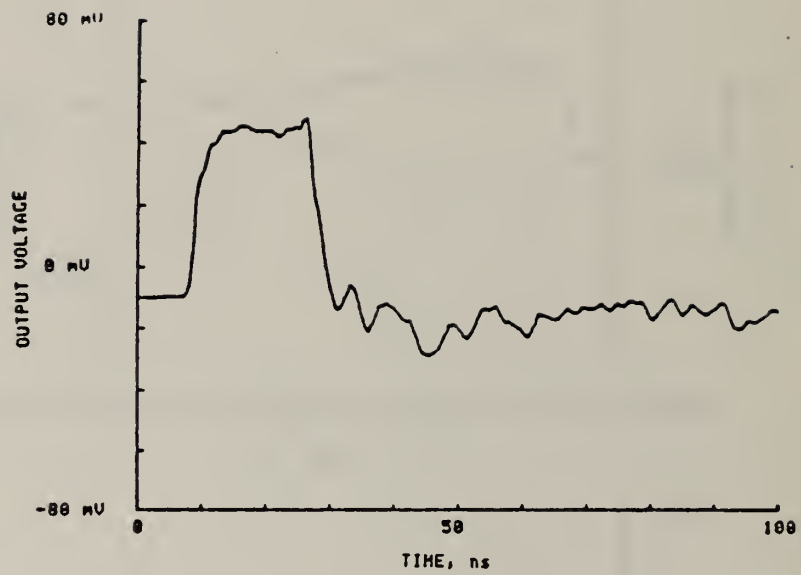
Figure 22. Output voltage from plug sensor in line. Signal input was from cable pulser, short cable (fig. 4).

the waveforms were identical. Only results for the flush mount are
shown here. Figures 23(a-c) show the waveform present at the end of the
transition section. Here the waveform exhibits an initial overshoot with
a number of subsequent oscillations. A signal with this signature is
characteristic of the response of many dividers to a voltage step. However,
what is observed here for all practical purposes is the actual waveform
exciting the probe. If the divider did have an oscillatory response, it
would have been present for the in-line signal as well (fig. 21). The
changes in waveform from the in-line to the end location are probably due
to the construction of the termination, which is a spider arrangement with
six legs, and the propagation of the wavefront in the extension. The
overshoot in the signal observed at the end of the line is seen on different
sensors and appears to be due to a complicated propagation mode in the
large extension, which results in some voltage enhancement. This overshoot
is also observed for high voltage pulses (see fig. 7). The results shown
in figures 21-23 and those below are typical of many measurements taken
for different charge cables, charging voltages, etc.

The BPA model sensor was mounted in the end of the·extension (fig. 3),
and the response was determined for different signals on the line, with
different low side configurations. A large number of records were obtained,
and those shown here have been selected to illustrate specific points.
The signals shown in figures 24(a-c) clearly indicate oscillations at two
frequencies (600 and 73 MHz). Although not obvious from the figures, the
magnitude of the signal is approximately 75 times greater than that
predicted by using the calculated ratio (table 1), and the measured charge
voltage. A similar result was reported in [14]. The data shown here are
for a minimum inductance low side capacitance. Figures 25(a-c) were obtained
with a single C_2, with greater inductance. The oscillatory character is not
changed significantly, but the output voltage is now some 360 times the
predicted value. These waveforms should be compared to those for the plug
sensor (fig. 23).

These responses show that the BPA sensor as configured in the laboratory
is not useful for measurements. An equivalent circuit described earlier
was developed which was used to explain the observations. The use of both
theoretical calculations and experimental results in understanding the
performance of various dividers is a critical element in developing optimum
divider configurations. The results of these calculations, which were
discussed in detail earlier, indicated that inductance in the circuit below
C_1 was responsible for the 73 MHz oscillation and the large signals. The
source of the 600 MHz oscillations has not been determined, but measurements
made with the disk sensor suggest that it may be an oscillation in the line
extension which couples strongly to dividers located above the ground plane.
This 600 MHz signal is barely discernable in the output of the plug sensor.
Changing the spacing of the BPA model sensor plate from 10 to 5 cm above
the ground plane did not modify the time dependence of the output in any
meaningful way.

To investigate the effect of damping in the divider, a 50 Ω resistor
was inserted between the sensor plate and the feedthrough, inside the extension.
Figures 26(a,b) show the waveform resulting from this modification. The
effect of the damping is obvious, but the overshoot is still significant,
and the divider is still unacceptable.
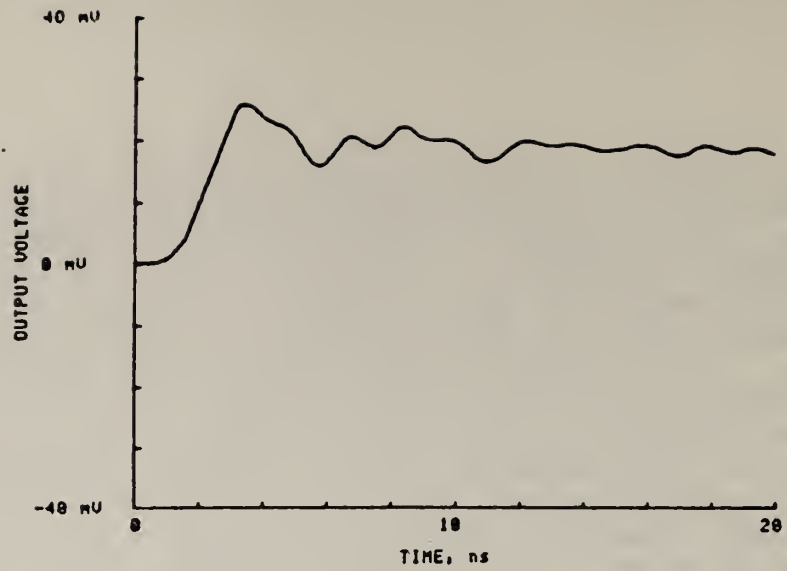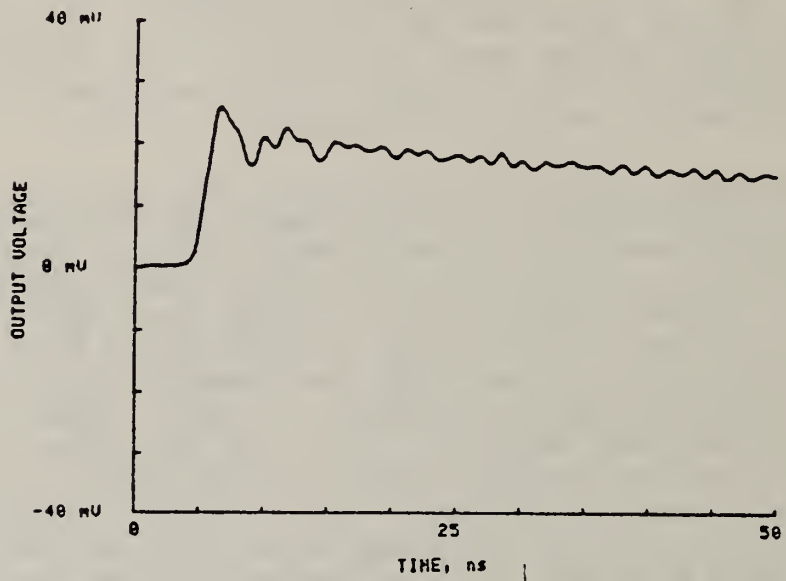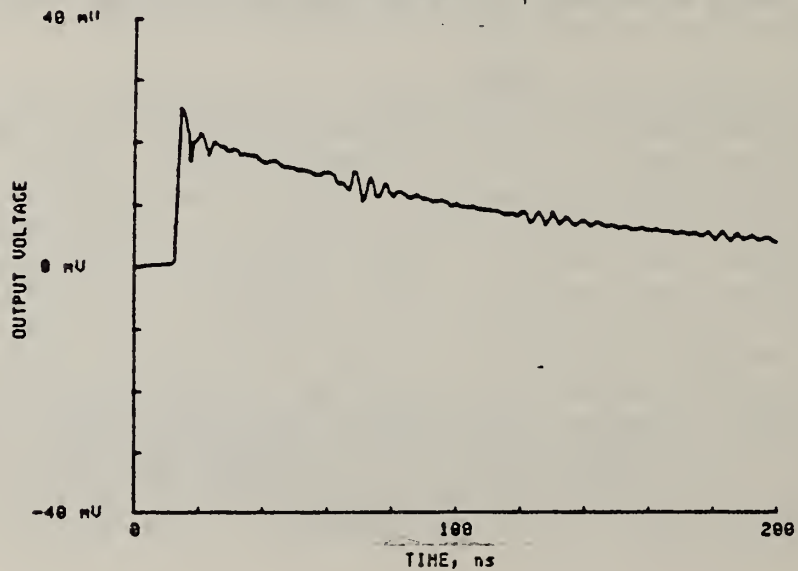
Figure 23. Plug sensor output voltage for sensor mounted at end of
extension line. Input signal, fig. 6.

34
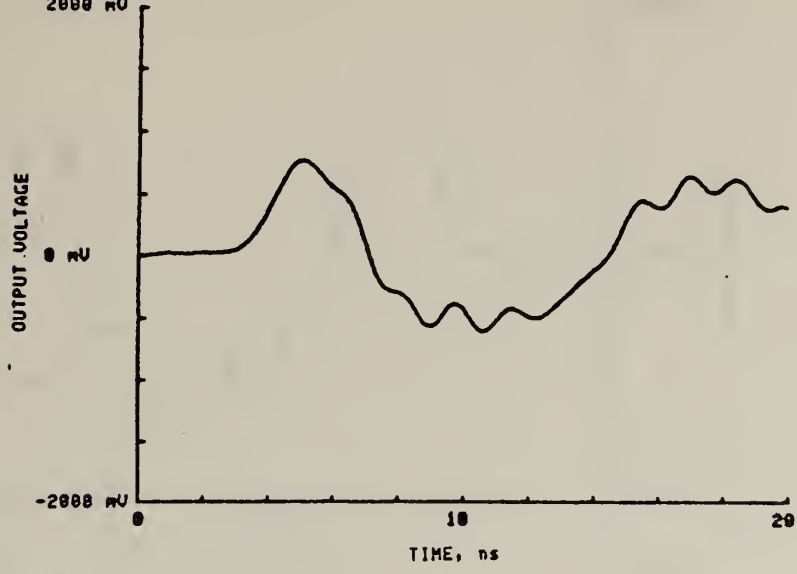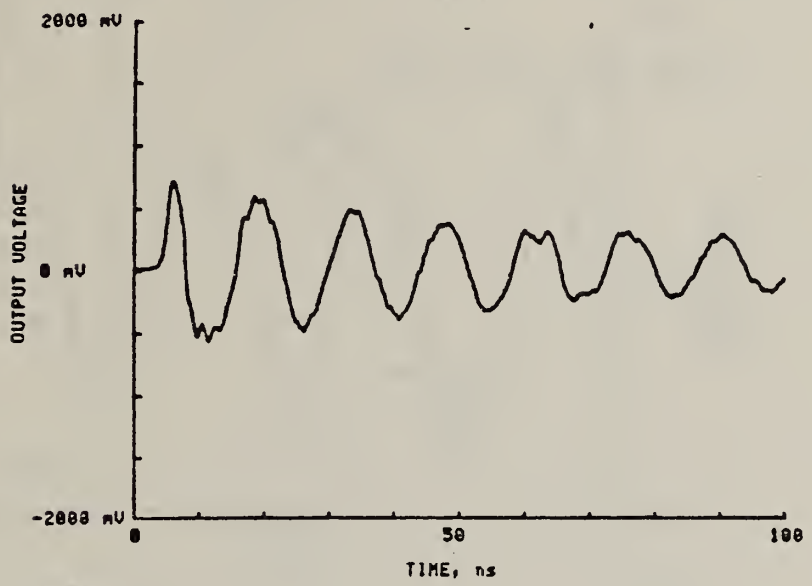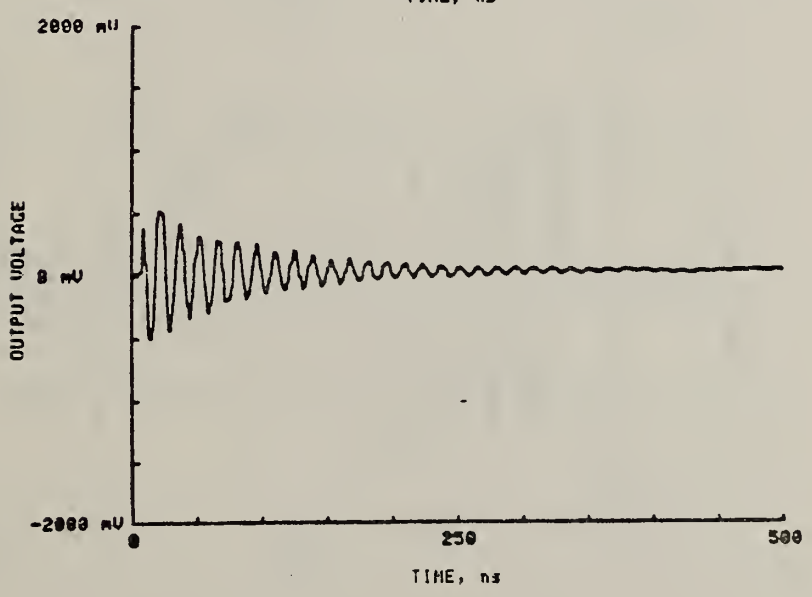
Figure 24.   BPA model sensor output voltage for distributed low side capacitance C_2 (see text).   Input signal, fig. 6.
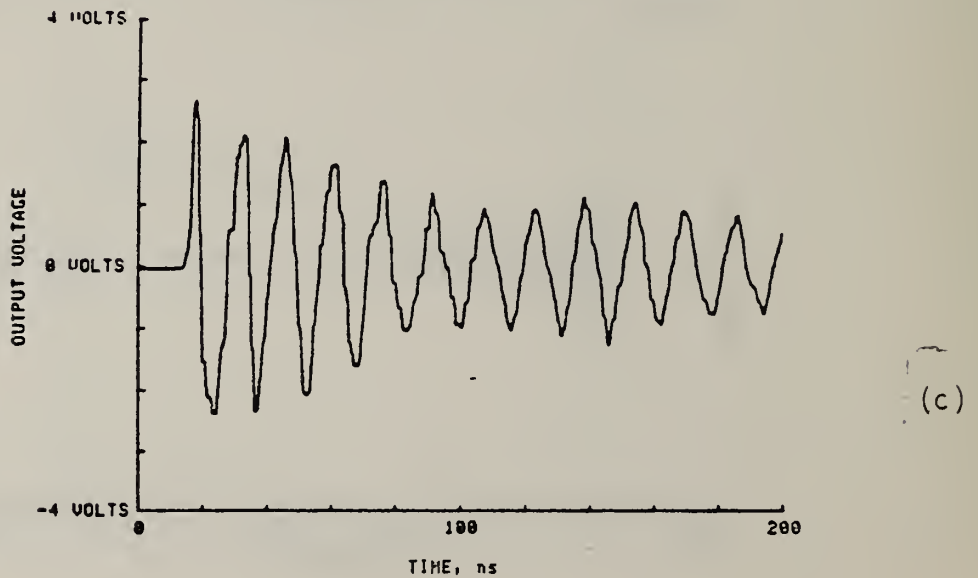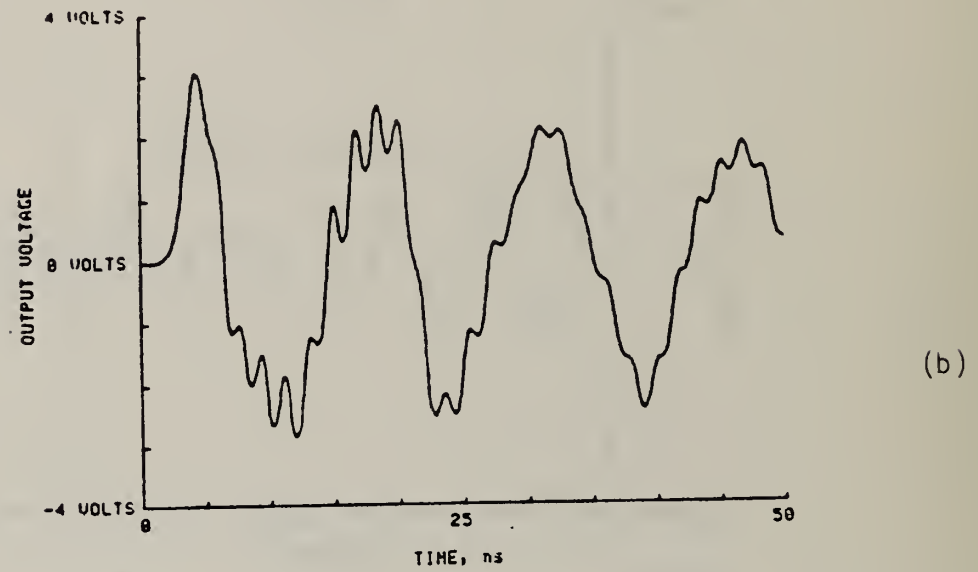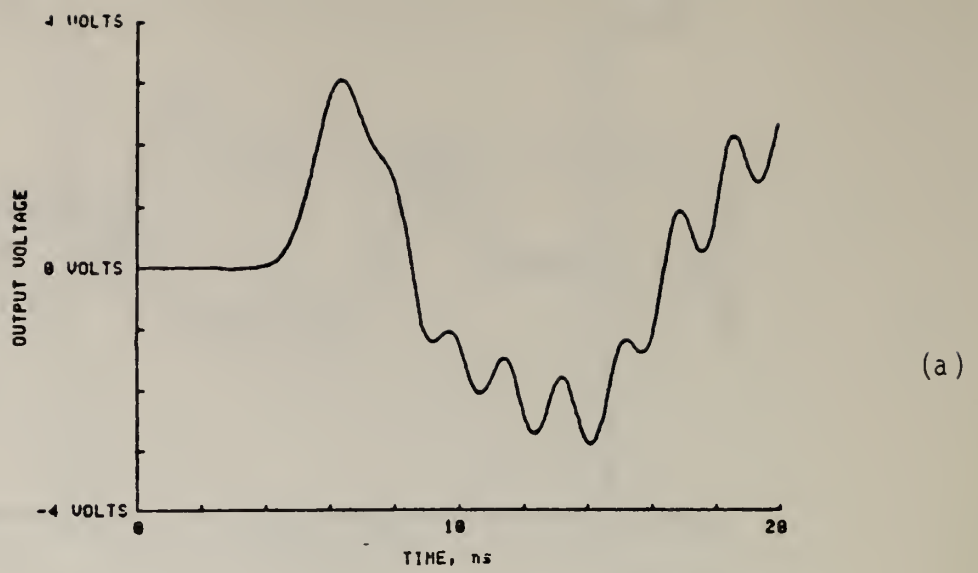
Figure 25. BPA model sensor output voltage for single capacitor low side (see text). Input signal, fig. 6.

36
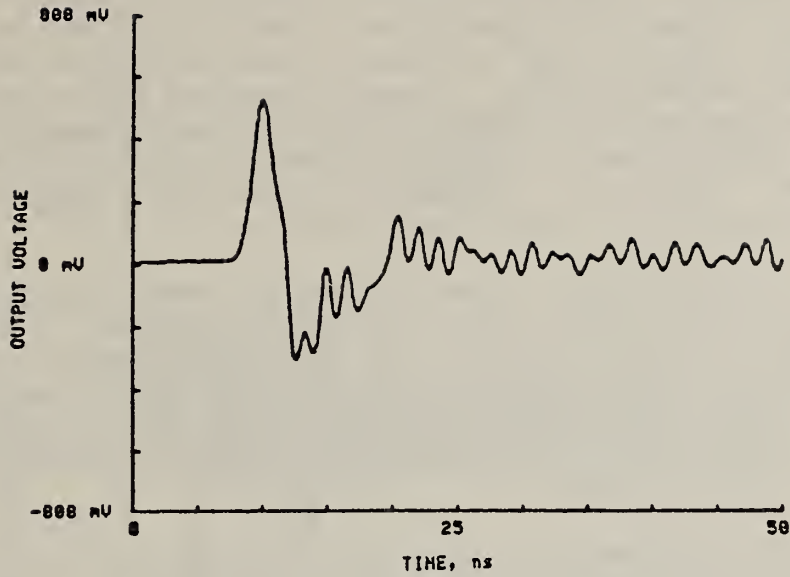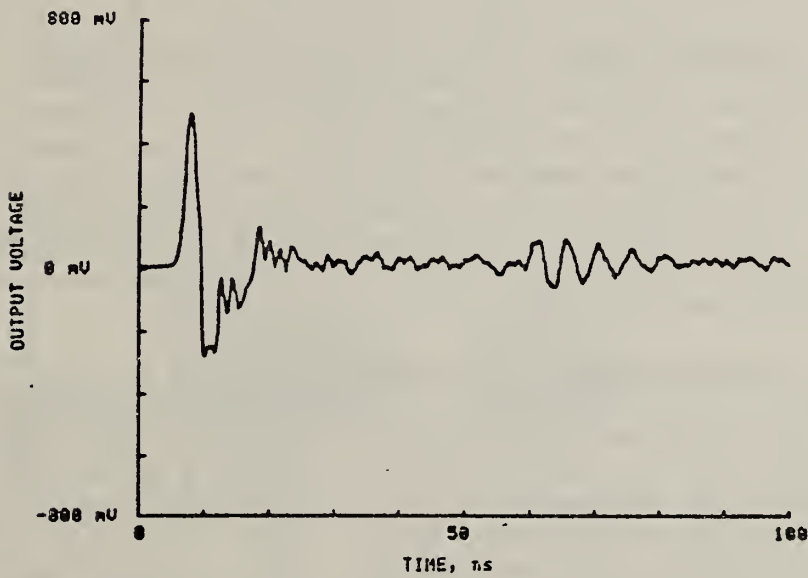
Figure 26.   BPA model sensor output voltage for distributed low side
capacitance C_2 and 50Ω damping resistance between C_1 and C_2.
Input signal, fig. 6.

Based on these results, the disk divider was designed and constructed. This design, with suitable engineering, could replace the BPA sensor with a minimum of modification to existing equipment. It was also used in determining the origin of the 73 MHz oscillation seen in figure 24. The disk divider could be mounted directly on the feedthrough used with the BPA sensor, or on standoffs on a mounting plate in which the signal connection was made to a type N bulkhead connector. As with the previous dividers, only records illustrating significant results are presented here. For signals shown in figures 27(a-c), the divider was mounted on 5 cm standoffs, and R_1 (fig. 14) was connected between the divider and the output connector inside the line. A coaxial grounded shield was positioned around R_1. When compared with figure 23 and figure 24, the difference is striking. The 73 MHz signal is gone, as expected, but the 600 MHz signal is still present. The output voltages are significantly lower for the disk sensor, although still larger than predicted.

Both the unshielded disk divider and the BPA sensor detected the 600 MHz signal, although their geometries were dissimilar. When the underside of the disk sensor, which is at dc ground potential, was shielded with a skirt, as indicated in figure 15, the signal was substantially reduced as is shown in figure 28. Experiments with improved shielding indicated that the oscillatory component of the signal seen in figure 28 could virtually be eliminated.

All of the results described above were obtained for low voltage, cable pulser-generated signals and no active electronics. Signals were also generated using the gas line and pressurized switch. In this mode, the system operated as a simple cable pulser which, in principle, would generate a 40 ns square wave of 10 kV amplitude for a 20 kV charging voltage. Charging voltages were measured with an electrostatic voltmeter. Examples of the waveform obtained are shown in figures 29(a-c), which were obtained with the plug divider. The overshoot at pulse onset and the oscillations observed on the wavetop are seen on the pulser-generated signals, indicating that they are real and associated with wave propagation through the switch assembly and in the extension. The signal rise time is excellent, which implies a low inductance in the switch itself. For these measurements, switch gas pressure was 0.219 MPa.

The outputs from plug and optimally shielded disk dividers can be compared directly, as in figures 30, 31, and 32, where the data shown were acquired for both pulser and high voltage signals. For the same input signal, the outputs are virtually identical. This is an important result, since it indicates that two sensors of significantly different geometries respond in the same way to the same signal. There is no significant distortion of the signal other than that predicted by eq (1). It also implies that the complex waveforms shown in figures 30-32 are indeed those exciting the sensors, and not a result of divider response.

In summary, experimental results show that the BPA sensor cannot be used to provide meaningful data regarding transients in gas-insulated equipment. Two alternative divider geometries have excellent transient characteristics, but both show the expected RC shaping which, without modification, limits their usefulness to transients with nanosecond duration.
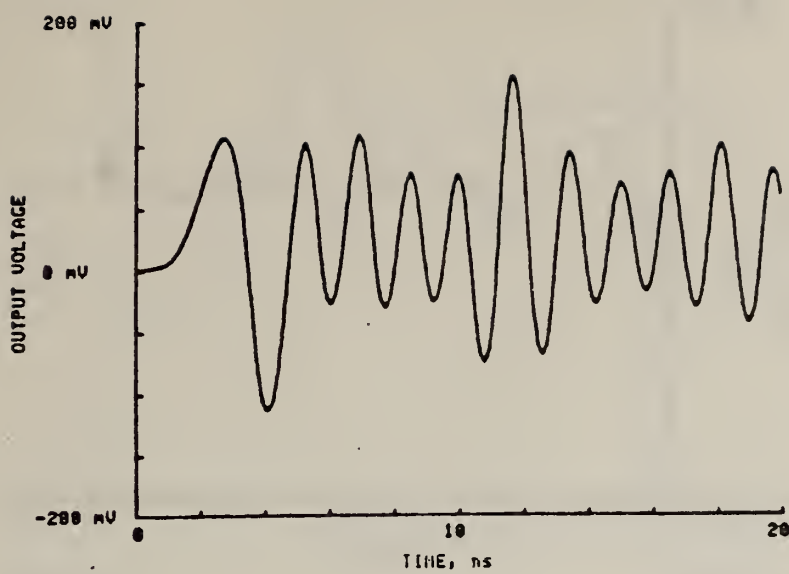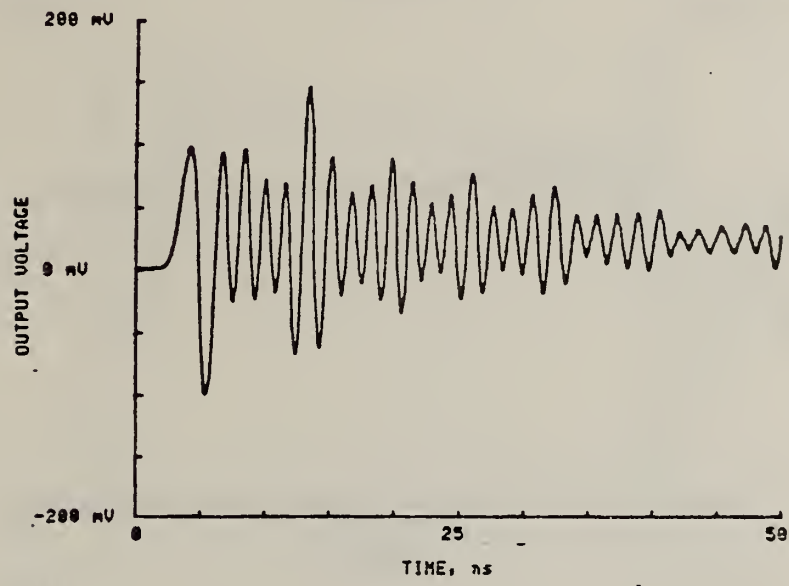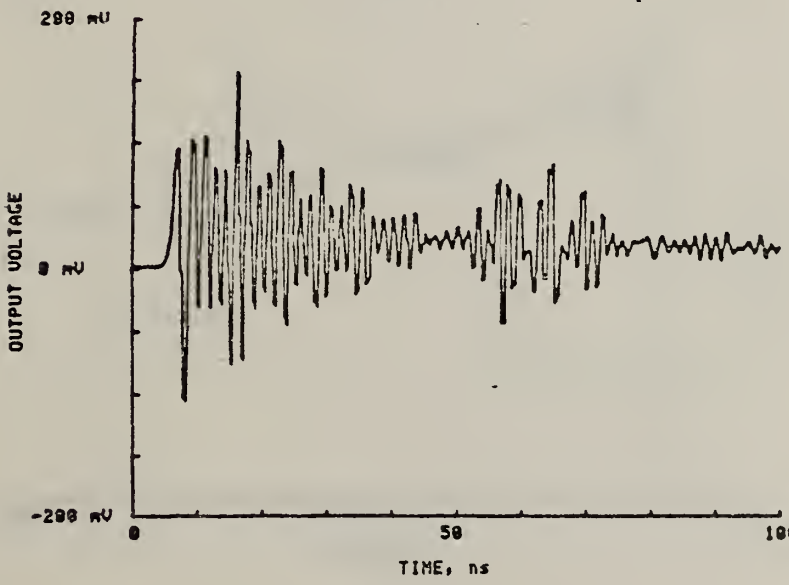
Figure 27. Voltage output from disk sensor mounted on 0.05 m standoffs, no shielding skirt (see fig. 15).

39
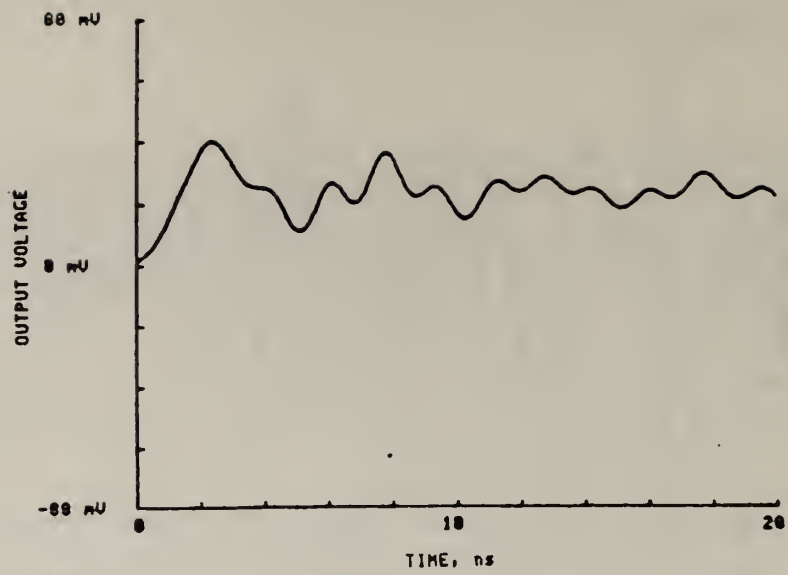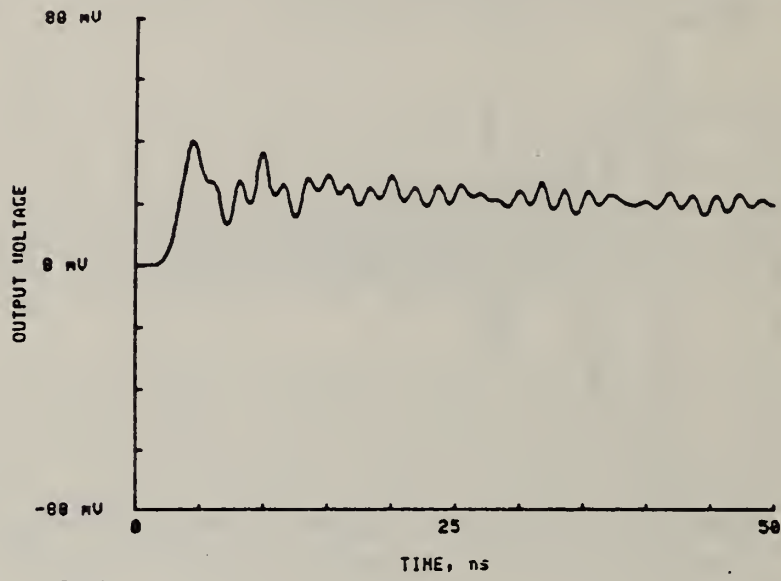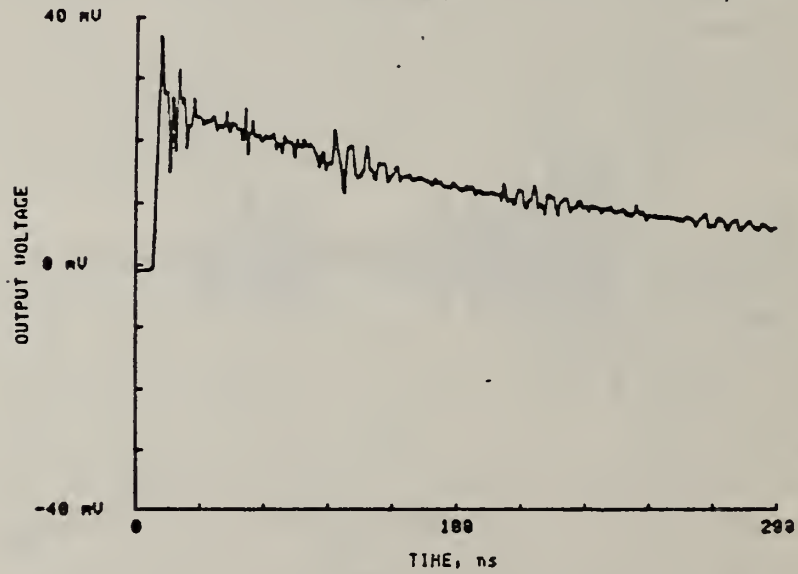
Figure 28. Disk sensor output voltage with shielding skirt (see fig. 15).

40
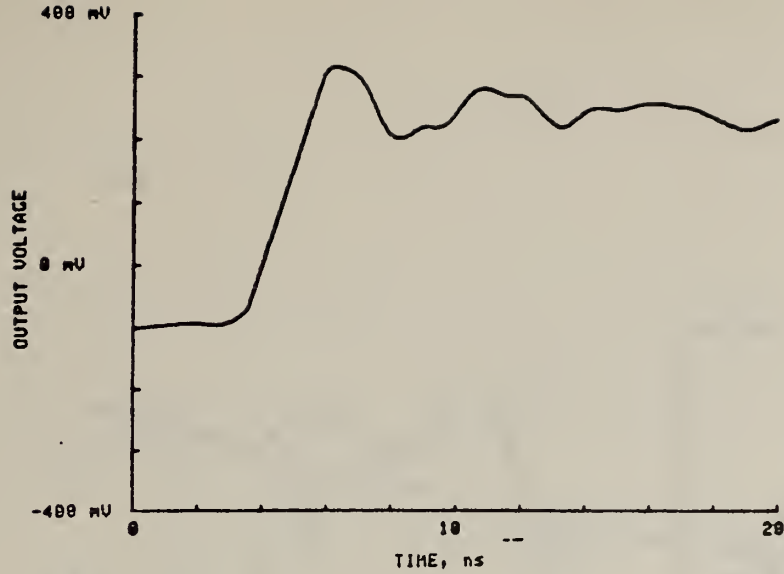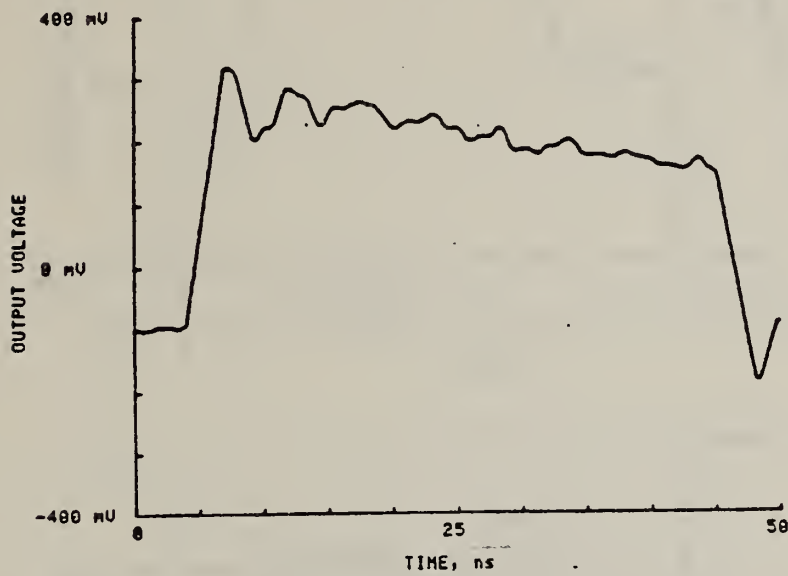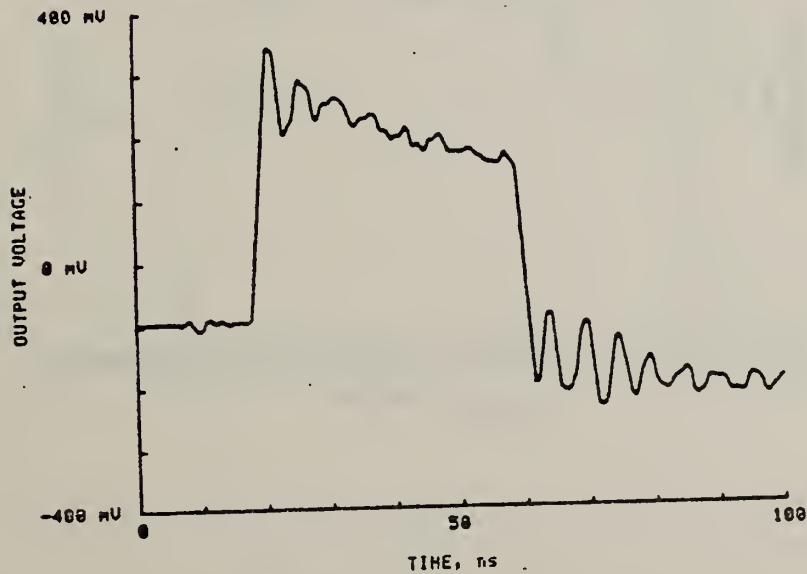
Figure 29. Signal from plug sensor mounted at end of extension for high voltage signal source. Line charged to 20 kV.
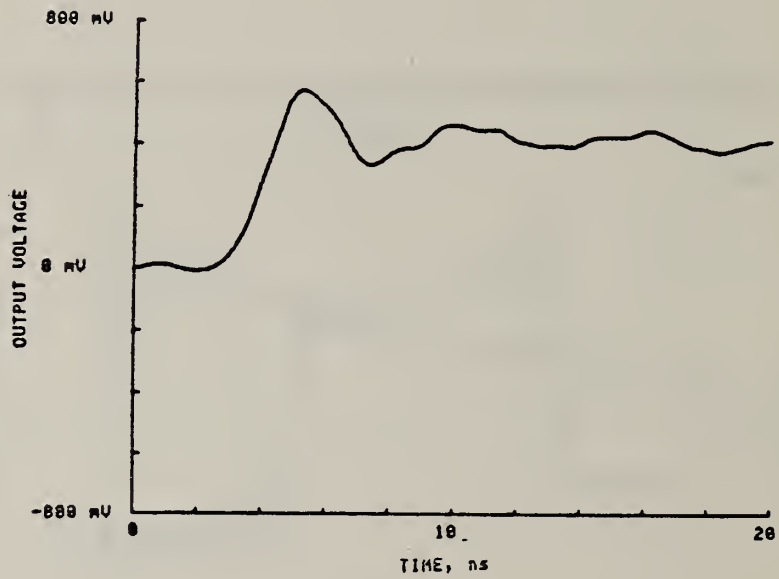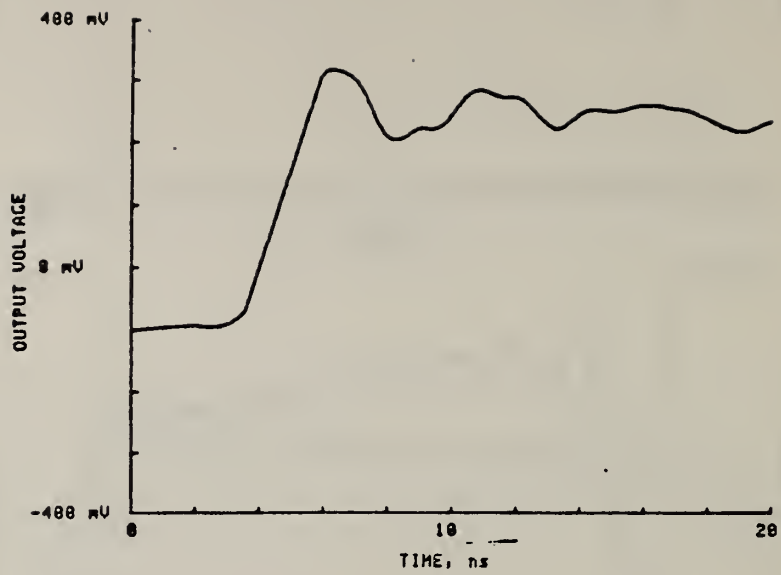
Figure 30.   Comparison of output voltage from plug sensor (a) and
disk sensor (b) for high voltage signal.
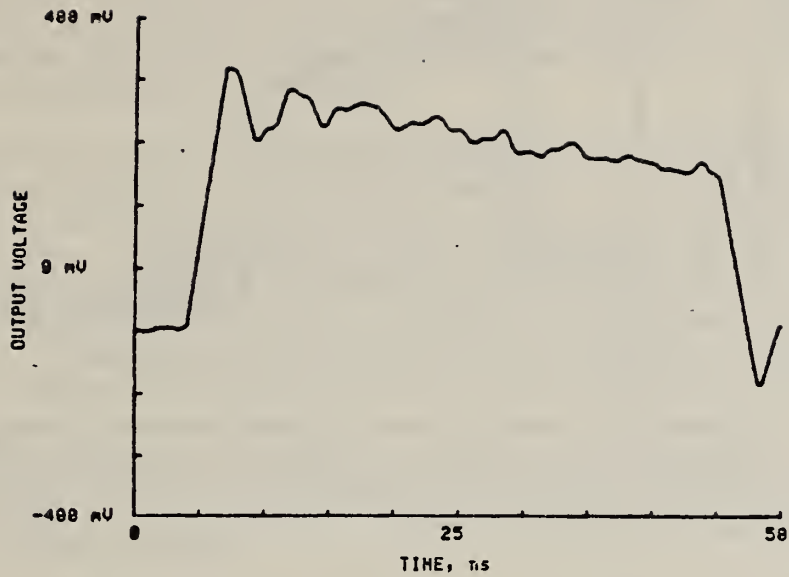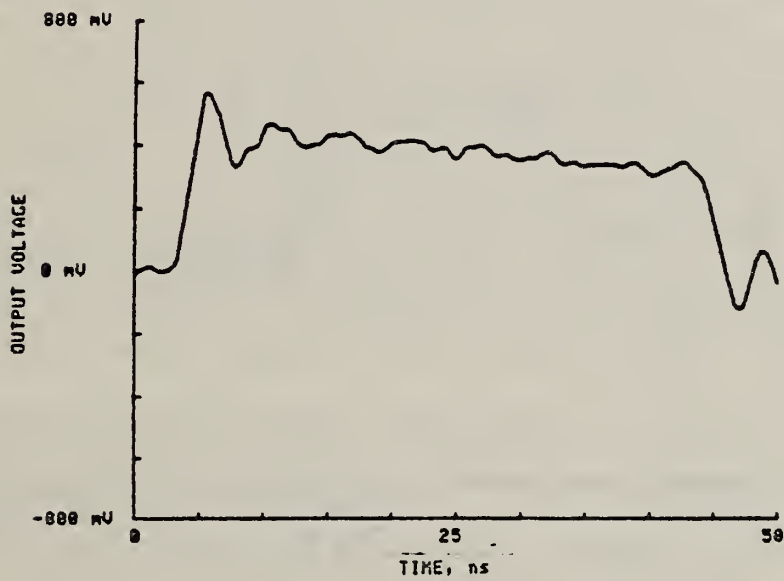
Figure 31. Comparison of output voltage from plug sensor (a) and disk sensor (b) for high voltage signal.
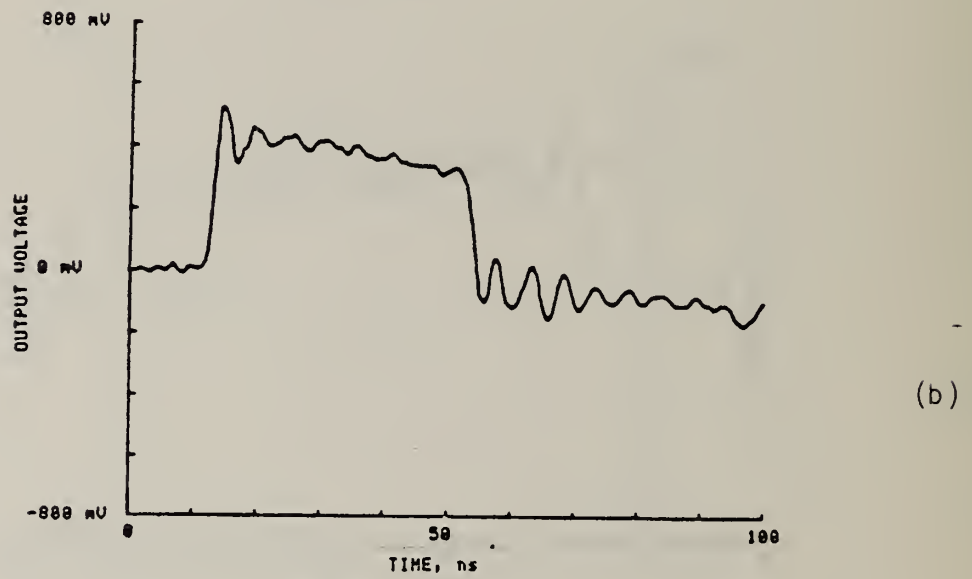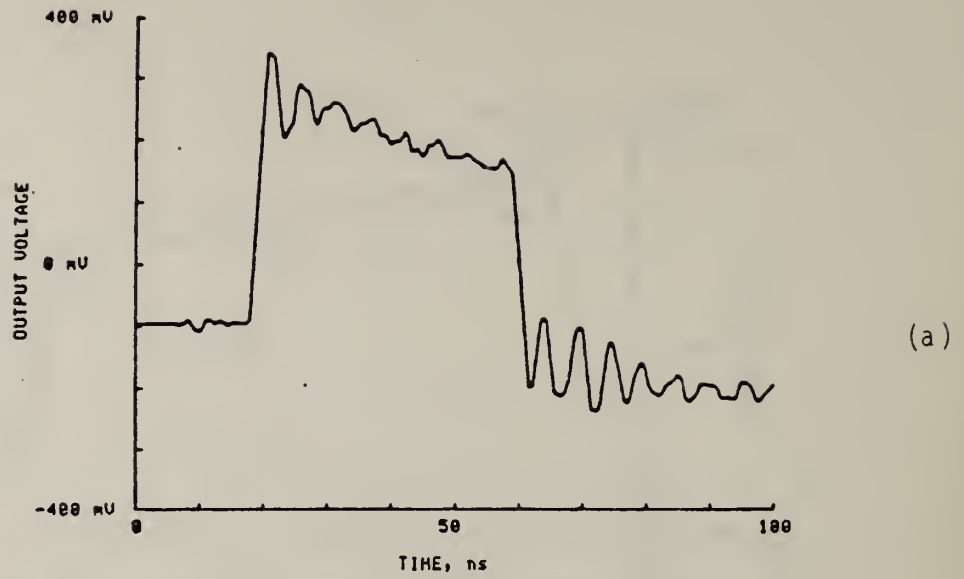
Figure 32.   Comparison of output voltage from plug sensor (a) and
disk sensor (b) for high voltage signal.

5. LINE DRIVERS AND OPTICAL LINKS FOR FAST PULSE TRANSMISSION

5.1 Line Drivers

As was discussed in earlier sections, the low frequency response of the capacitive dividers can be extended by orders of magnitude by using high input impedance active electronics at the output of the divider. These electronic devices, in turn, will be characterized by some bandwidth and rise time so that the system response will be a composite. Care must be exercised in mating the active probes to the capacitive sensor to ensure that no spurious responses are produced.

Three different active systems were evaluated in the laboratory and two of these were used with sensors described earlier. Two wide-band active probes and a fast buffer amplifier were tested for possible use as a fast-pulse coaxial cable driver. (As mentioned later, these units may also be suitable for modulating the transmitter in fiber optic telemetry links.) These devices were first tested with input voltage steps obtained from a commercial pulse generator. Measurement and storage of all waveforms from the above equipment were made with the digitizer system described in earlier sections.

Figures 33(a-c) show a voltage step from the pulse generator applied directly to the digitizer using three different sweep speeds. The specified rise times (10-90%) of the digitizer system used and pulse generator are 0.8 and 3.5 ns, respectively.

Figures 34(a-c) show the effect on these waveforms of inserting a commercial FET probe (probe A) between the pulse generator and digitizer. This probe has unity gain, 100 kΩ input impedance, a rise time of approximately 0.4 ns, and is capable of driving a 50 Ω load with signal levels up to ±600 mV. A long signal cable (150 ft of RG214/U) was also used between the probe output and the digitizer. The attenuation of high frequencies in the cable is indicated in figures 35(a,b) which show the decrease in rise time caused by inserting 150 ft of RG214/U coaxial cable between the probe output and digitizer. The attenuation of this cable at 50, 100, and 200 MHz is approximately 2, 3, and 4.5 dB, respectively. While not a problem in the present work, the effects of long cables on fast signals can be important. Computer corrections can be made for this signal distortion [26].

Figures 36(a-c) show the system response when a different commercial probe is inserted between the pulse generator and digitizer. The second probe (probe B) has a 10/1 attenuation, a 10 MΩ input impedance, and a 0.7 ns rise time. Figure 37 shows the effect of inserting the long RG214/U cable between the probe output and digitizer. In figures 36(a-c), the voltage scale reflects the input voltage levels to the probe.

An alternative to using commercial FET input probes is to use a fast buffer amplifier. These amplifiers have bandwidths greater than 100 MHz, slew rates up to 6000 V/μs, and have been used in fast pulse measurements [27]. These amplifiers were examined for their usefulness in the present investigation.[1]

Figures 38(a-c) and 39(a,b) show the system responses when a buffer amplifier is substituted for the probe. For these measurements, a 3.74:1

_____

[1]Special circuit boards based on this design were kindly supplied by
 Glen McDuff, Texas Tech University, Lubbock, Texas.
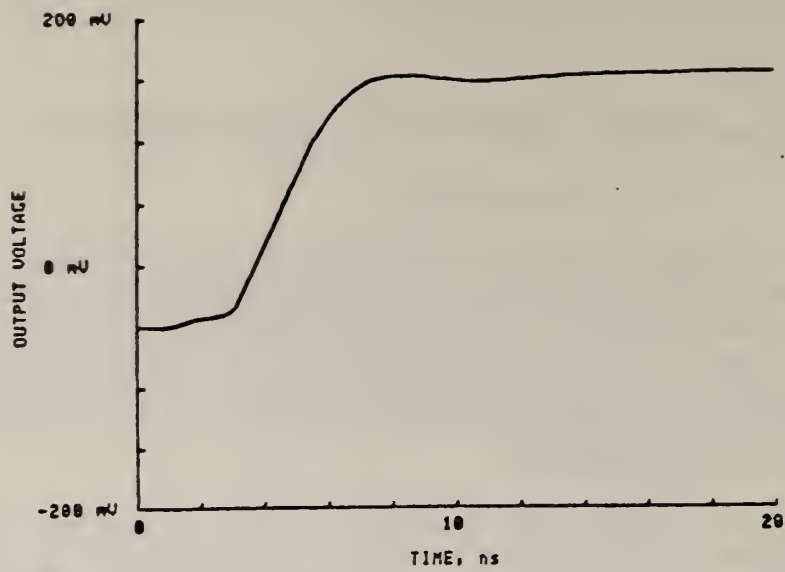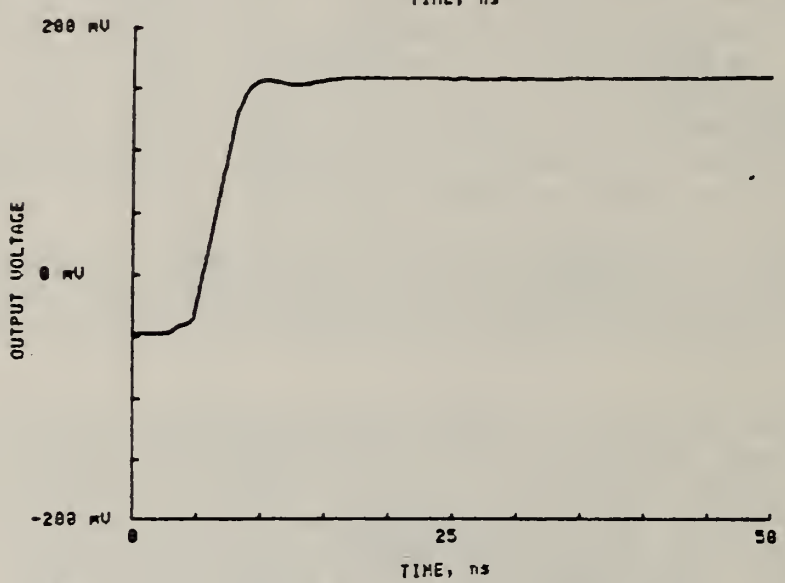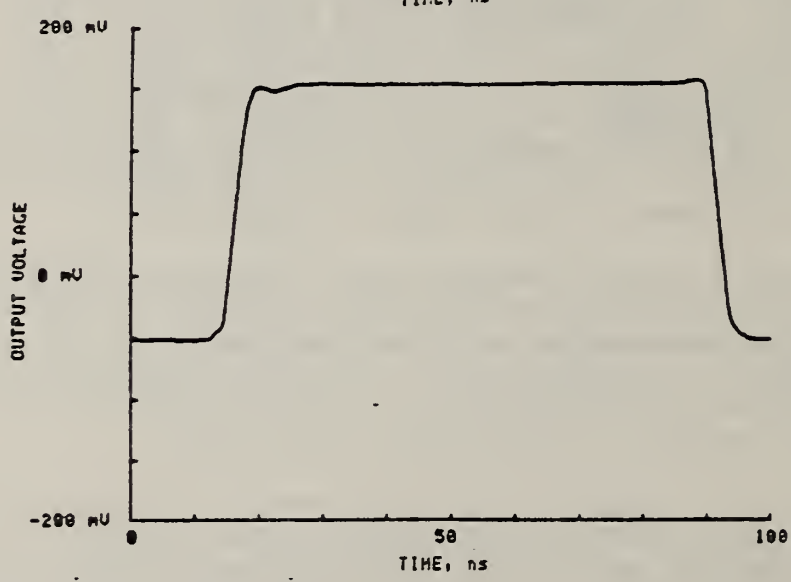
Figure 33. Output signal from pulse generator used in evaluating low side electronics.

46
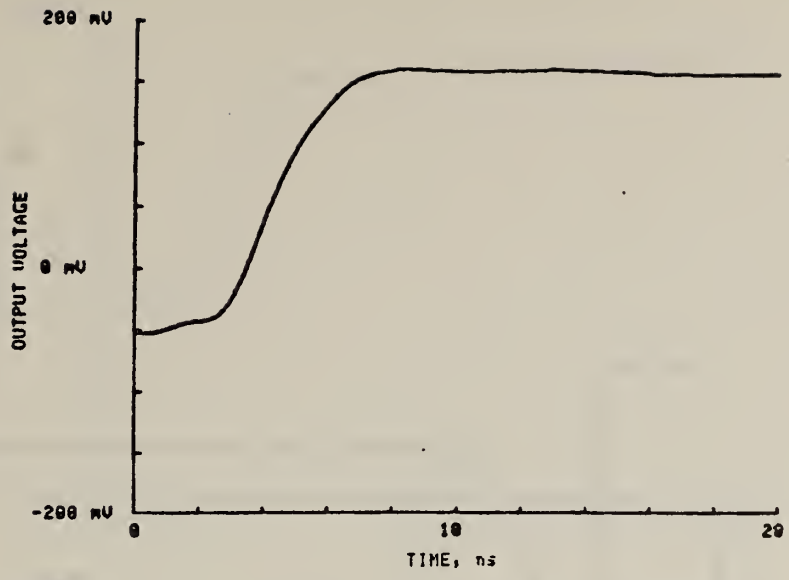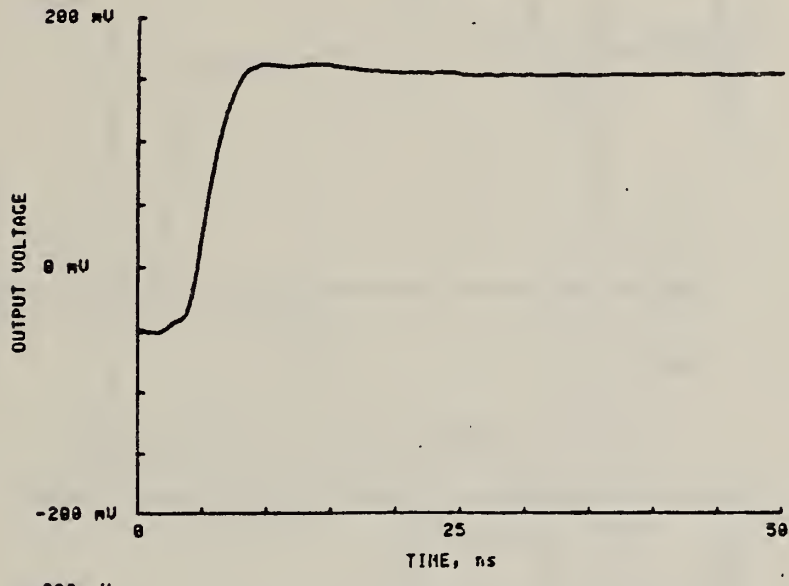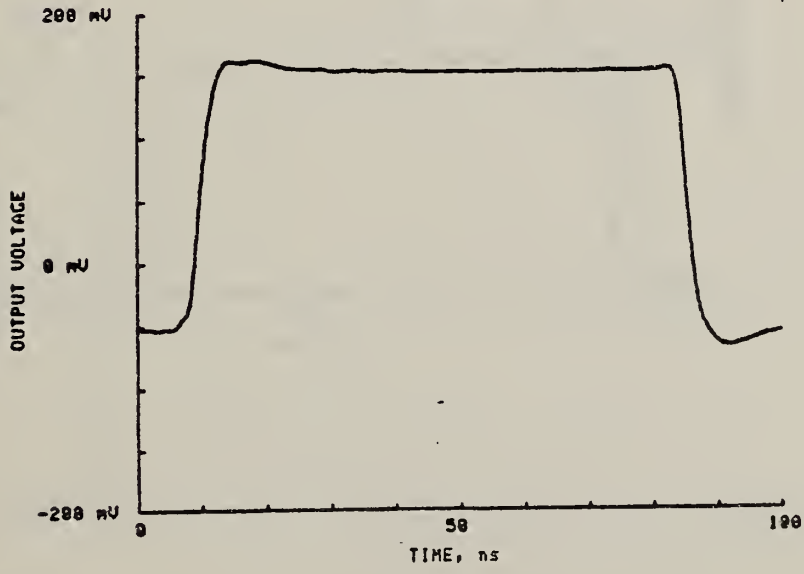
Figure 34. Output signal from probe A (see text) driven by signals shown in figure 28.
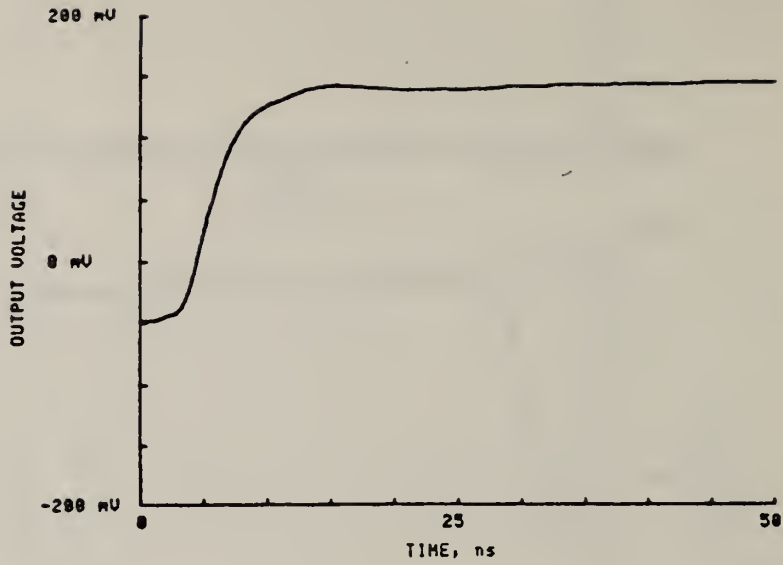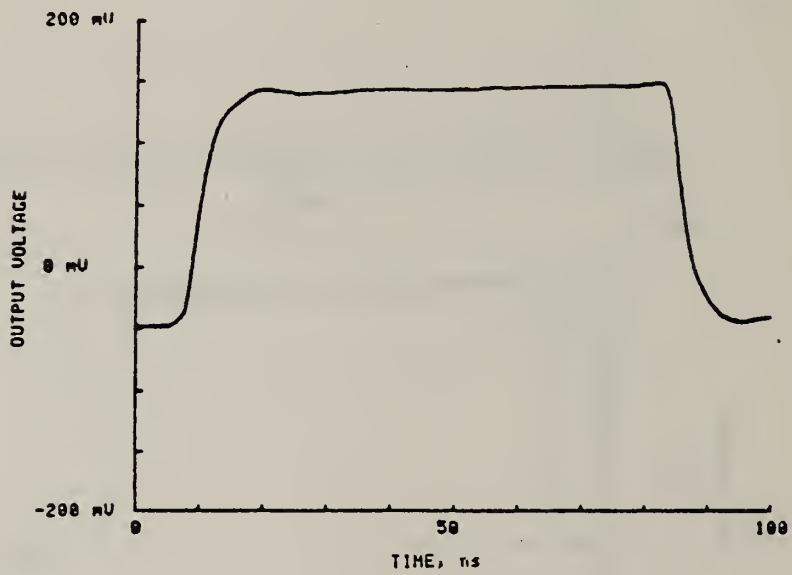
Figure 35. Output signal from probe A driving 46 m of RG214/U.

48
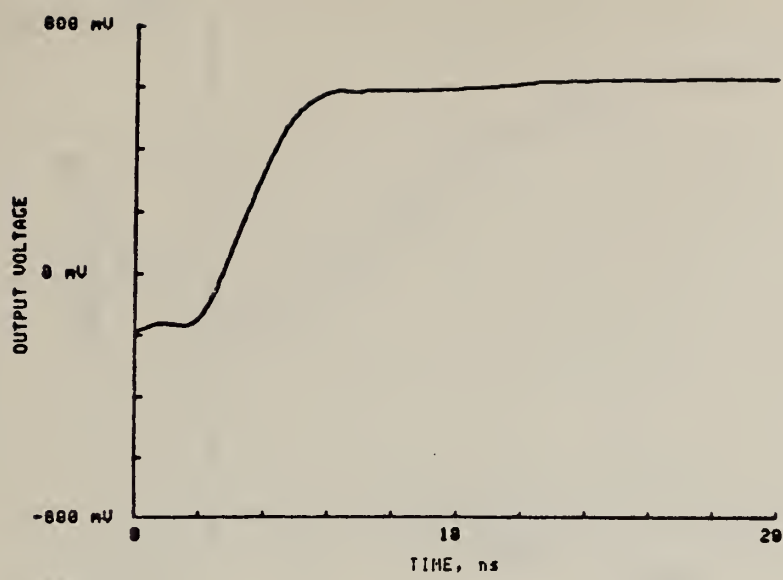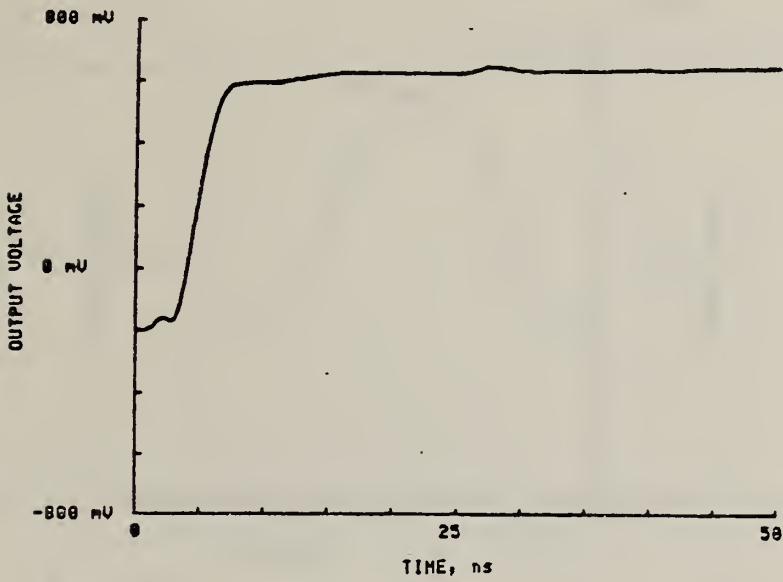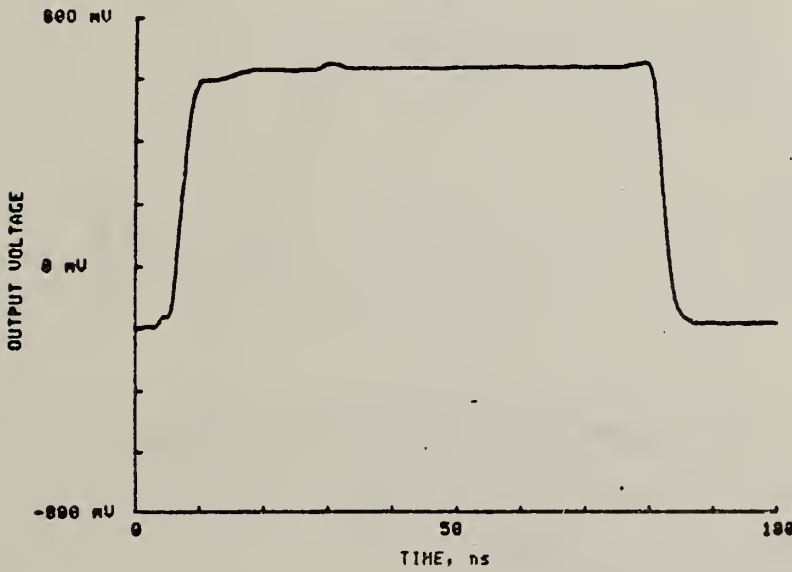
Figure 36.   Output signal from probe B (see text) driven by signals shown
             in figure 33.   Short output cable.
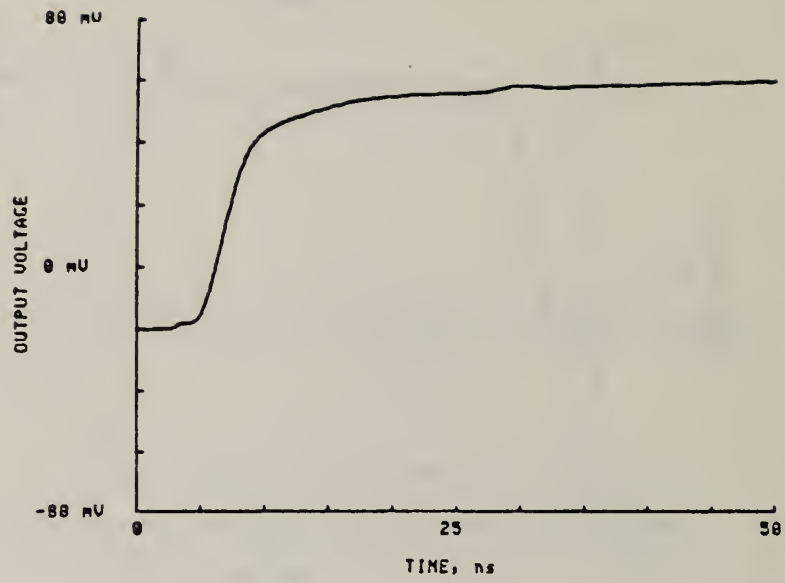
Figure 37. Output signal from probe B when driving 46 m of RG214/U cable.
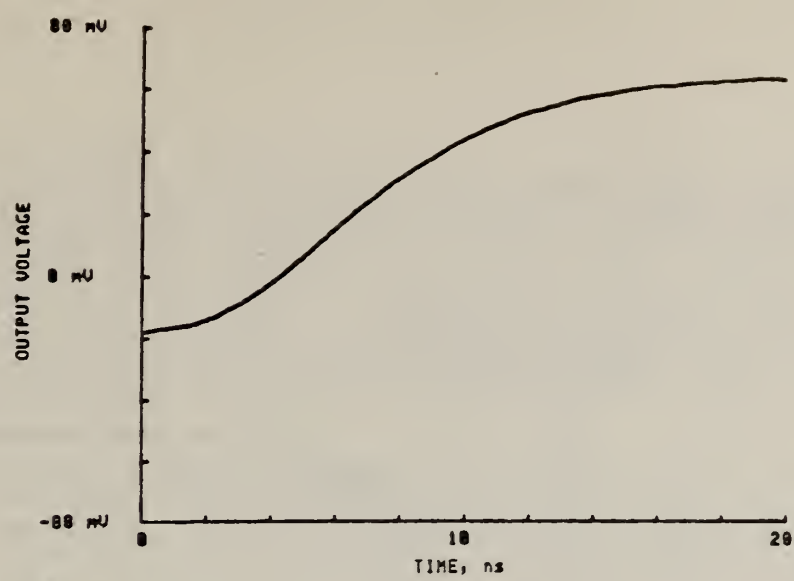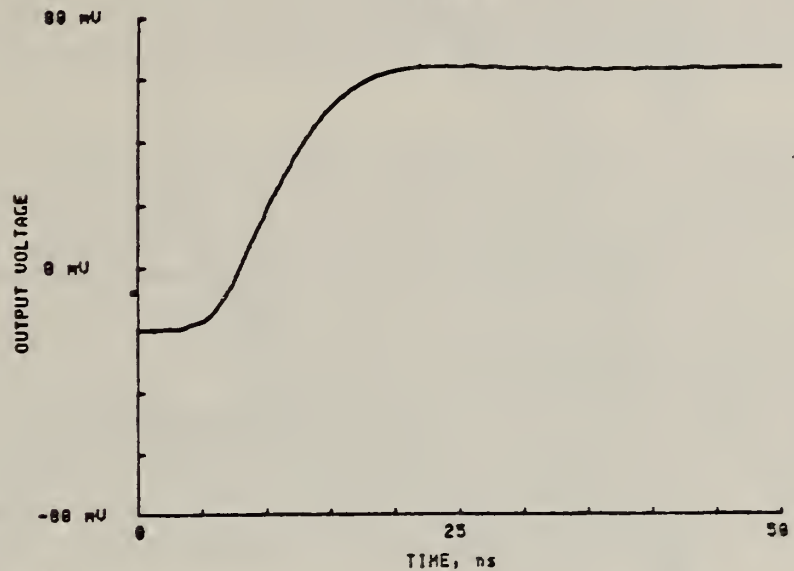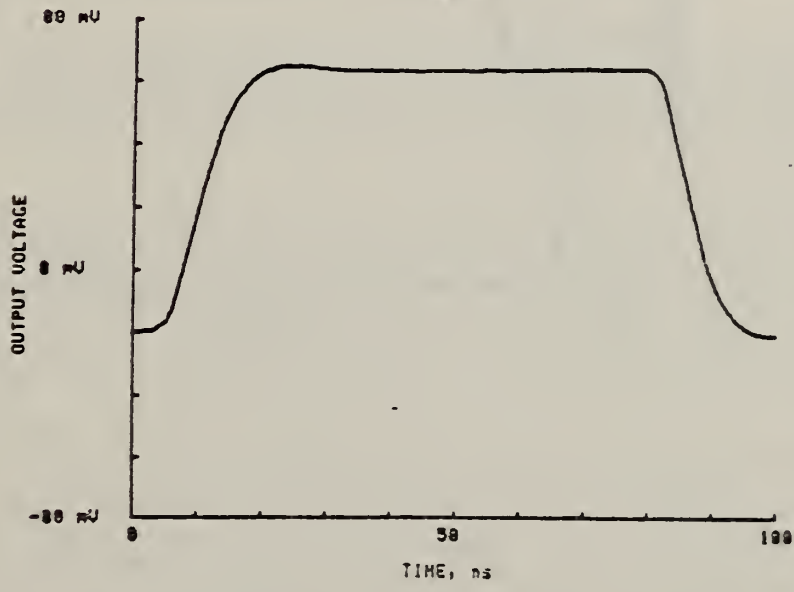
Figure 38.   Output signal from fast buffer amplifier when driven directly
from pulse generator (fig. 33).
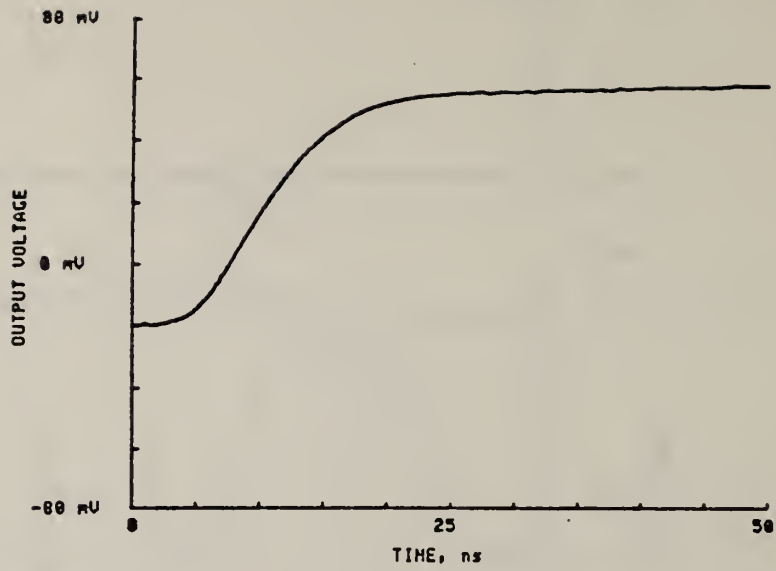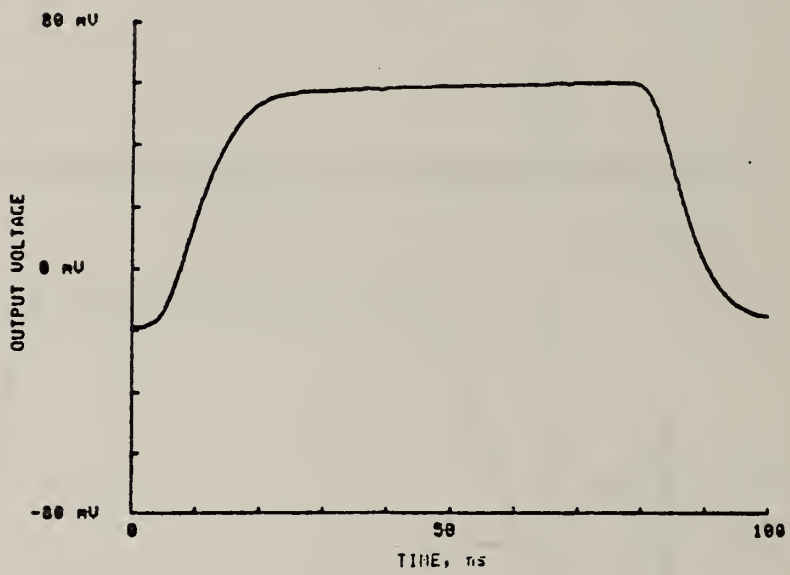
Figure 39.   Output from fast buffer amplifier driving 46 m of RG214/U cable.

attenuator (13.65 MΩ impedance, shunted with 2.2 pF capacitance) was added
to the input of the amplifier to minimize the overshoot characteristic of
this amplifier. Since the input capacitance of amplifiers with series
feedback usually increases with frequency in the upper range of their frequencies,
overshoot in these amplifiers can often be decreased by suitable choice of
capacitor values in an input attenuator. A capacitor ratio of ~3.74 was the
smallest ratio that could be used to minimize overshoot in the amplifier
employed in these measurements. Hence, the choice of 3.74 for the attenuation.

Comparisons of waveforms shown in figures 29(a-b) and 31(a-c) with those
in figures 28(a-c) show that both commercial probes are suitable as cable
drivers, subject to the output signal level constraint of ±600 mV on probe A.
Depending upon the input signal level, the 10:1 attenuation of the second
probe may be undesirable. Also, the relatively low input impedance (100 kΩ)
of the first makes this probe less useful as it limits the low frequency
response of the composite systems.

Combining the rise times of the pulse generator and buffer amplifier in
root-sum-of-squares fashion yields a rise time of about 8 ns for the buffer.
As indicated in later measurements, when the amplifier was used without an
input attenuator, the rise time decreased with increased overshoot.

Tests were next conducted using the model gas-insulated transmission
line illustrated in figure 2. The signal was produced using the mercury-
wetted pulser described earlier. The voltage of the inner conductor was
measured using the NBS plug sensor shown in figure 13. Figure 40(a) shows
the result of a measurement of the sensor output, using probe B, while
figure 40(b) shows the sensor output connected in a passive mode. Because
of the divider action of R_1 and R_2 (fig. 14) there is a factor of 2
difference in the signal levels between figures 35(a) and 35(b).

A comparison of figures 40(a) and 40(b) indicates that the probe reproduces
perturbations in the model line reasonably well. Similar results were obtained
for probe A. Figures 41(a,b) and 42(a,b) show the plug sensor output waveform,
employing the probe B for the sweep speeds used in previous measurements.

Figures 43(a,b) show the response of the buffer amplifier when fed by
the plug sensor, using the same connecting cable used in all of the previous
measurements. It is believed that the considerable amount of ringing was
largely caused by the long lead path between the sensor output (starting
at the top of R_1, fig. 13) and the input terminal of the amplifier. This
path included an adapter for connecting between N- and BNC-type connectors.

To evaluate the buffer amplifier when placed integral to a capacitor
sensor, the amplifier circuit board was mounted in the disk sensor at the
location of R_1 (fig. 15). The sensor output electrode (C_1) was connected
directly to the buffer input with a very short lead. Also, since the
signal level was only 22 mV (44 mV open-circuit), the 3.7:1 attenuator was
removed and a 10 MΩ resistor connected from input to ground. The ground
plane of the circuit board was connected to the sensor ground electrode
and the connector ground with pairs of short copper straps. The ±15 V power
supply voltages were each filtered on the amplifier circuit board by two 0.1 μF
ceramic capacitors and a 4.7 μF solid tantalum capacitor. Further filtering
of these voltages was provided by feeding the power supply leads into the
sensor package by 0.001 μF ceramic feedthrough capacitors and a ferrite bead.
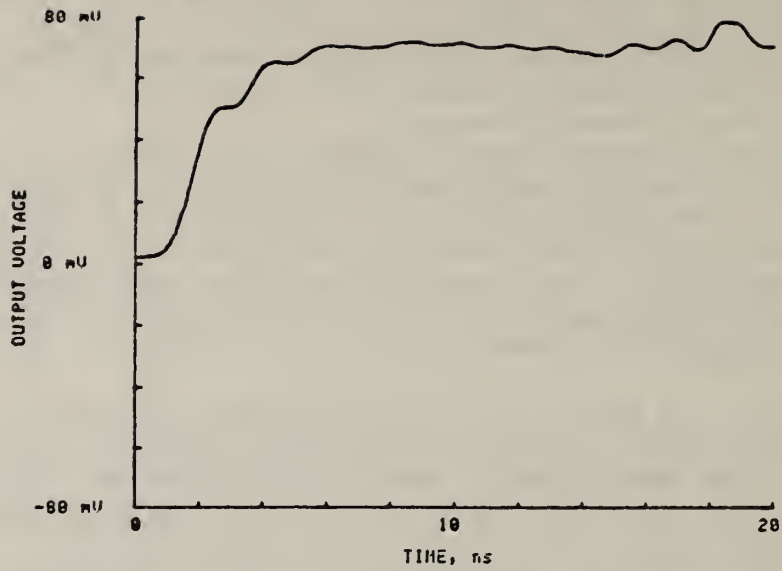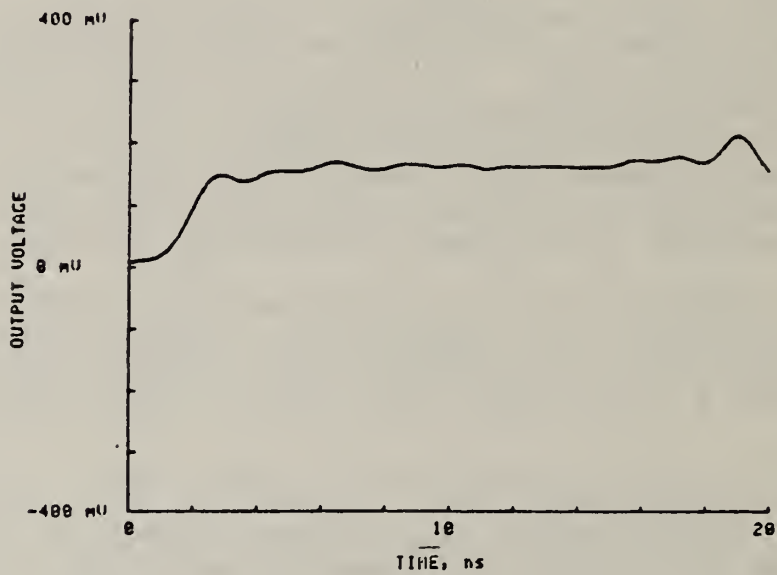
Figure 40.   Comparisons of measurements of signals on the gas line
             for the plug sensor located in-line operated passively
             (a) and with active electronics (probe B) in the low
             side (b)
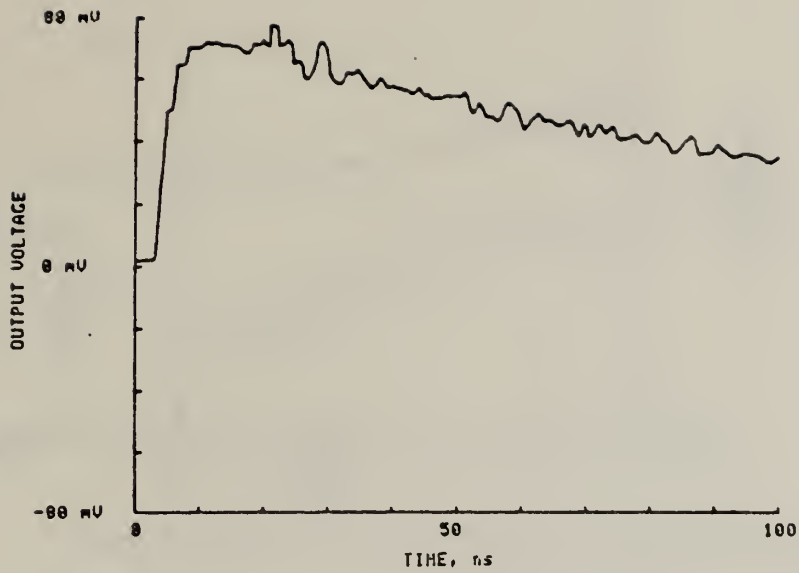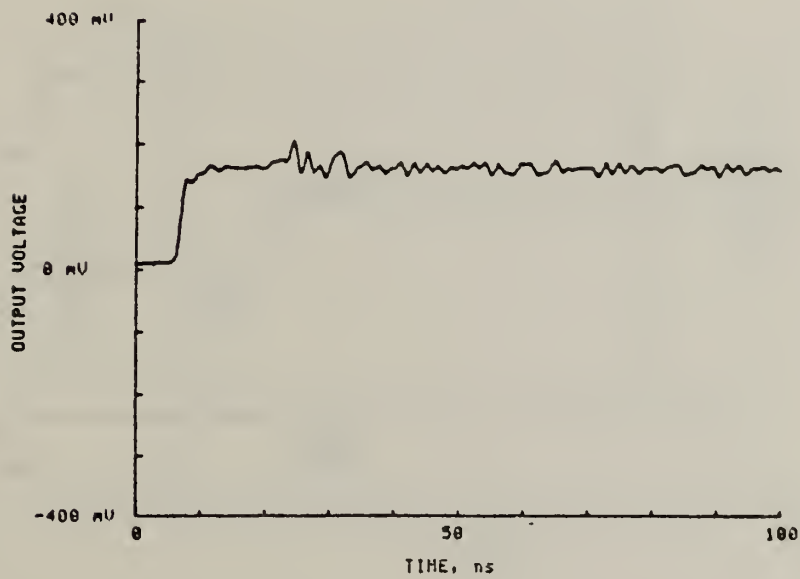
Figure 41. Comparisons of passive (a) and active (b) low sides (see fig. 40).
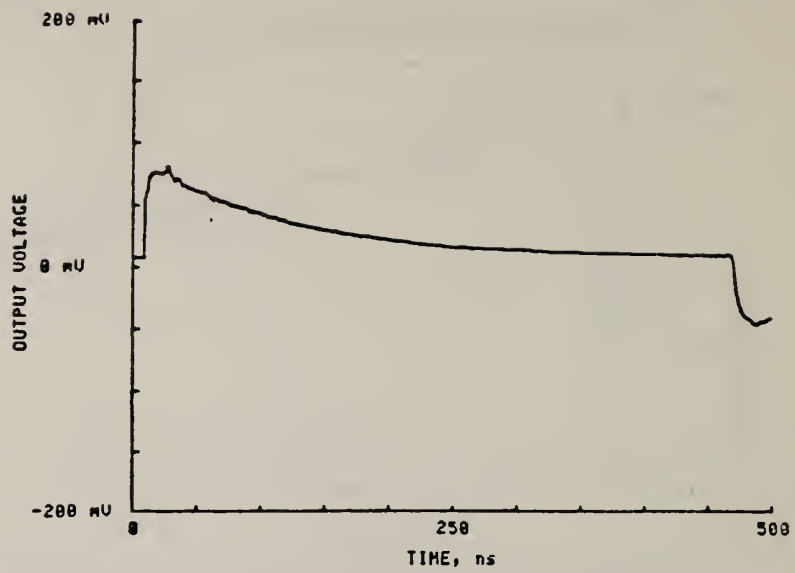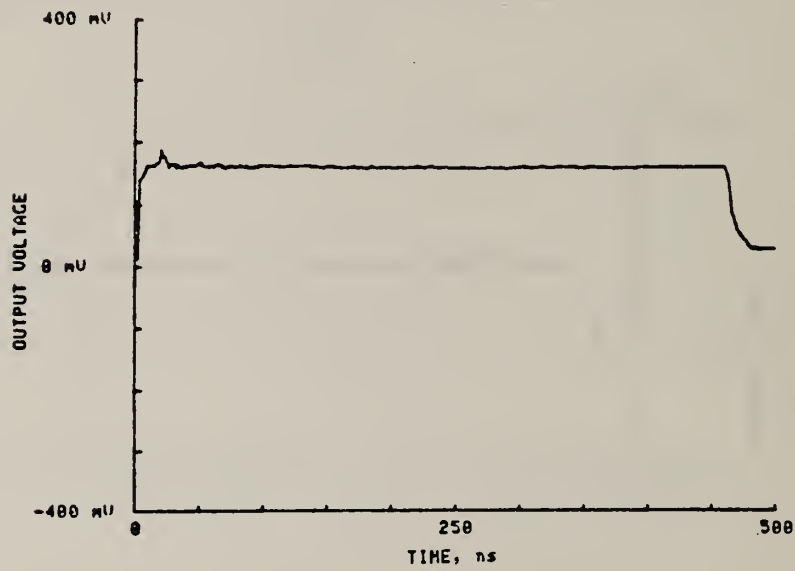
Figure 42. Comparisons of passive (a) and active (b) low sides (see fig. 40).

56
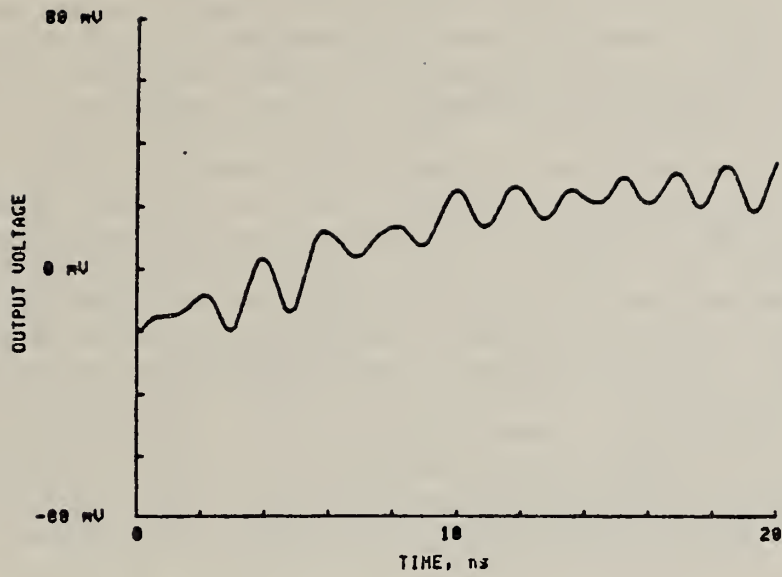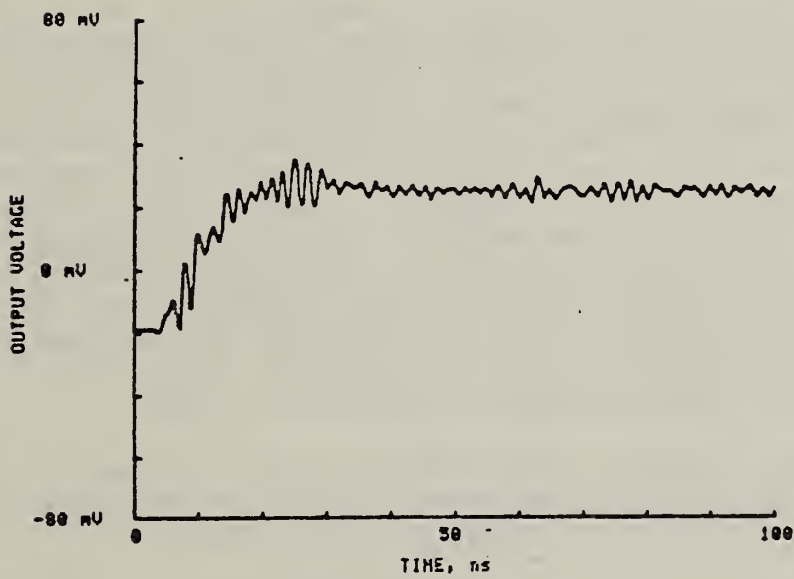
Figure 43. Output signal from fast buffer amplifier coupled to output of plug sensor located in line.

Figures 44(a) and 44(b) show the output waveform from the buffered disc sensor. Based on previous measurements made on the unattenuated buffer amplifier (not shown), approximately two-thirds of the overshoot shown in those figures is attributable to the amplifier. When compared with figure 28, the decrease in rise time and the loss of high frequency detail is obvious.

5.2 Optical Links

The chief advantages of the fiber optic telemetry links over coaxial cable links are their immunity from electromagnetic interference and the small loss of signal strength and bandwidth when the signal is transmitted long distances. Fiber optic telemetry links may generally be classed as either digital or analog systems. This discussion is limited to analog systems employing an amplitude modulated light-emitting diode (LED) or a laser diode as the transmitter element. The detector used at the receiving end of these systems is usually a PIN diode or an avalanche photo diode (APD). Since the detector is a current source, a transimpedance amplifier (current-to-voltage converter) must be used with the detector to provide a useful output. In most systems, the detector-amplifier bandwidth determines the system bandwidth. The detector-amplifier bandwidth can be maximized by using a low gain amplifier. This is feasible if a large optical signal is received, or if the detector sensitivity is large. Avalanche diodes have one to two orders of magnitude greater sensitivity than PIN diodes and, therefore, facilitate the design of wideband receivers. Their disadvantages are a gain-dependence on temperature, high noise, and high cost.

The modulator of the transmitting element (LED or laser diode) must provide peak-to-peak drive currents ranging up to at least ±10 mA, usually capacitively coupled to a 50 Ω load. The modulator bandwidth should be sufficiently large to have minimal affect on the system bandwidth. Continuous laser diodes are favored over LEDs for wideband applications because of their higher power output and faster rise times. The narrow spectral linewidth of lasers (2-4 nm, as compared to approximately 50 nm for LEDs) is important to minimize fiber material dispersion if the length of the fiber cable is larger than about 100 m. The disadvantages of laser diodes, relative to LEDs, are their current dependence on temperature, poor linearity, and higher cost. The first two disadvantages can be minimized by careful regulation of the base-value current (an additional cost) and utilizing a small percent (depth) of modulation (<50%).

Fiber optic telemetry links (complete systems) range in price from approximately $500 for a 25 MHz system to $4000 for a 200 MHz system. Prices up to $20,000 are quoted for the 200 to 500 MHz range.

It is not known whether the modulator (or input amplifier) of any of the wideband commercial transmitters can be directly interfaced with a capacitor-divider type of sensor, such as the NBS disc sensor. Therefore, it may be necessary to employ a special amplifier for interfacing between the sensor and the transmitter. Possibly, one of the probes or the amplifier, evaluated for coaxial cable driver use, could be used. The telemetry system bandwidth requirements, along with the signal level requirement of the waveform measuring and recording equipment, will determine the receiver requirements.
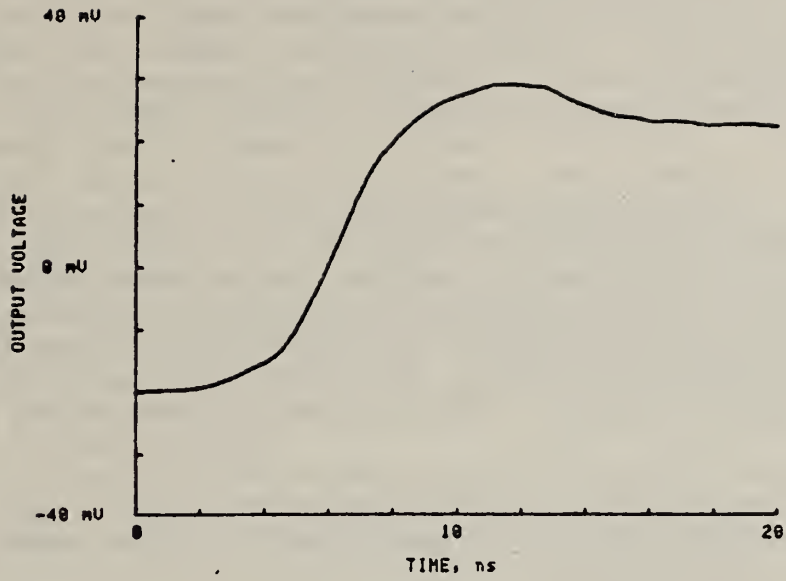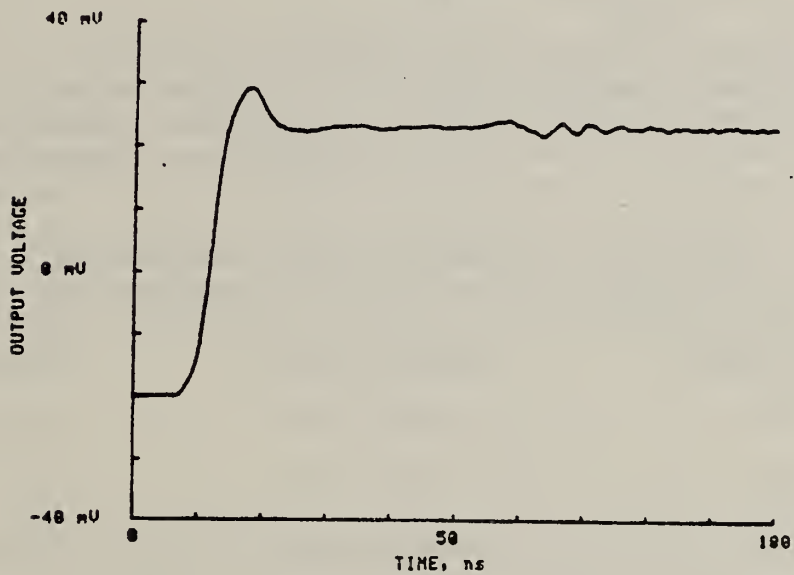
Figure 44.   Output signals from fast buffer amplifier installed integral
to disk sensor (see fig. 15, text).   Signal on test line was
produced by mercury-wetted relay pulser.

6. CALIBRATION

Although the transient response of the dividers can be studied in the laboratory, their ultimate application is in field installations. The high voltage capacitor C_1 (fig. 17) does not exist as a discrete component and its value depends on the geometrical relationship between the divider assembly and the high voltage electrode. In a properly designed divider, this should be the only difference between laboratory and field installation. In the laboratory, a three-terminal bridge measurement may be used to determine C_1. Such a measurement may only be practical in the field during installation. In either case, the value of C1 is small, on the order of 1 pF. For the plug sensor, bridge measurements were made for C_1 and C_2 (fig. 17) for the in-line location. The ratio in table 1 is based on these capacitance measurements. The experimental ratio determined from the step response for a number of different measurements is shown in table 3. There is some disagreement between the two. However, there are systematic errors associated with the experimental numbers. One of these errors has to do with the mismatch at the transition between the pulser output and the gas line. This mismatch will result in a reflection which will reduce the transmitted pulse below its theoretical value. This error is in a direction consistent with the observed discrepancy. There are small losses in the signal cable.

No individual calibrations were made of the digitizer or the FET probe. As a result, the uncertainty of the experimental values of the ratio may be as large as ±10%. With this consideration and those stated above, the agreement is reasonable.

One procedure proposed to allow determination of C_1 in the field is to compare the divider output at 60 Hz with a calibrated voltage sensor, say a potential transformer. In principle, everything about the divider system except C_1 is known, once it has been evaluated in the laboratory. This procedure has some severe problems, as can be shown by a theoretical analysis.

Table 3. In-line plug sensor measurements

Measurements	Measured ratio[a]	Calculated ratio[b]
(1)	4.02×10^{-4}	4.57×10^{-4}
(2)	4.20×10^{-4}	4.57×10^{-4}
(3)	9.02×10^{-4}[c]	9.14×10^{-4}
(4)	8.91×10^{-4}[c]	9.14×10^{-4}
(5)	4.09×10^{-4}	4.57×10^{-4}
(6)	4.17×10^{-4}	4.57×10^{-4}

[a]Based on actual voltage measurements.
[b]Based on measurements of circuit parameters.
[c]Measurements (3) and (4) were made with the FET probe. As noted in the text, this changes the effective divider ratio by a factor of 2.

Using the equivalent circuit of figure 17, frequency response was calculated using component values for the plug sensor. Both low impedance and high impedance values were used for R1 and R2 to reflect the use of passive or active low side signal handling. No consideration was given to the low frequency response of the active low side probes, although this would enter into an actual calibration. These results are tabulated in table 4. It is clear that the passive mode would not be usable in the lab, because of the enormous ratios involved. Very small inductances, which are negligible at 60 Hz, can cause significant deviations from a pure capacitive behavior at high frequencies as is shown in figures 45 and 46. These step responses were calculated for high impedance R1 and R2. The change in step response due to 1 nH is significant, resulting in an initial transient overshoot of approximately 60%.

In the laboratory, there are calibration problems as well, but they are more readily addressed than in the field. In principle, it should be possible to calculate the magnitude of the transient propagating through the test facility, if the characteristic impedances of each section are known. This approach is less reliable than a direct measurement, but should be investigated more thoroughly, since the combined use of impedance information and a transient code, such as EMTP, may yield adequate information with a minimum investment effort.

It is important to carefully define the level of accuracy required for any given measurement. Based on this level, an error budget for the entire measurement process can be given and resources allocated appropriately. Based on the work reported here, as well as that of others, there should be little difficulty in achieving adequate time response to avoid temporal distortion of electrical signals in the kilohertz to several hundred megahertz range. However, an adequate means of achieving amplitude calibration has not been demonstrated.

Methods used to calibrate voltage sensors in large pulse power systems are described in [19]. Two methods are discussed, both of which require access to deenergized equipment. Although useful for comparison, these methods do not appear to have applicability to the present problem.

61
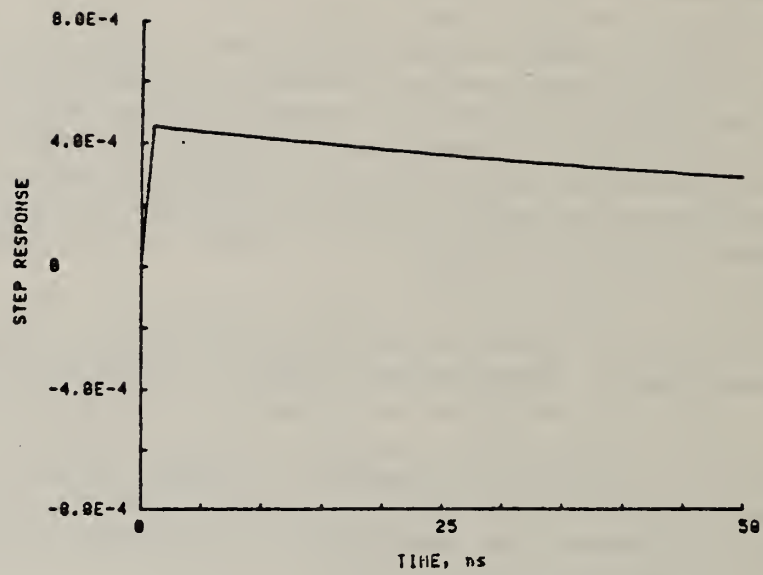
Figure 45. Step response calculated for plug sensor using circuit in figure 17 and component values C_1 = 1.01 pF, C_2 = 1107 pF, R_1 = 50 Ω, R_2 = 50 Ω, and all other components negligible.
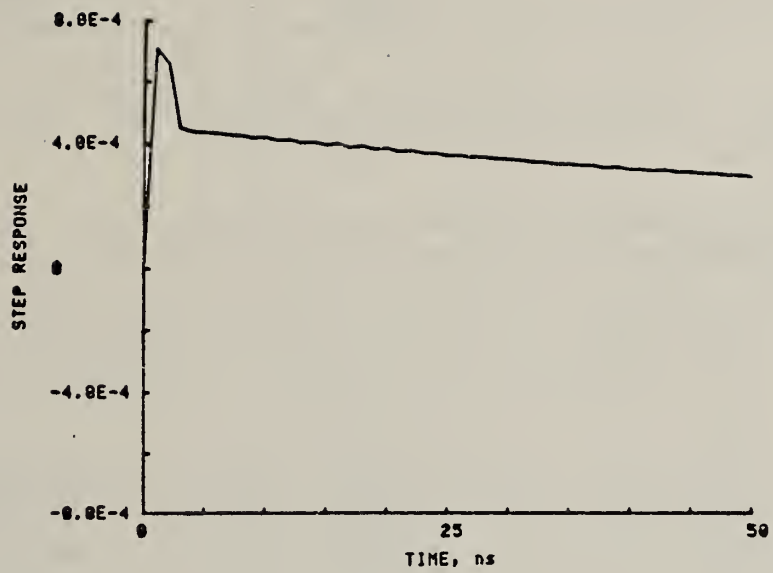
Figure 46. Step response calculated for plug sensor using component values listed in figure 45, except $L_g = 1$ μH (see fig. 17)

Table 4. Calculated ac response for plug sensor

Freq. (Hz)	V_o/V_{in}[a]	V_o/V_{in}[b]
6.0E + 1	1.904E – 8	1.904E – 8
6.0E + 2	1.904E – 7	1.904E – 7
6.0E + 3	1.904E – 6	1.904E – 6
6.0E + 4	1.902E – 5	1.902E – 5
6.0E + 5	1.757E – 4	1.757E – 4
6.0E + 6	4.432E – 4	4.426E – 4
6.0E + 7	4.556E – 4	3.840E – 4
6.0E + 8	4.558E – 4	6.808E – 3

[a] C_1 = 1.01 pF, C_2 = 1107 pF, R_1 = 50 Ω, R_2 = 50 Ω
All other components are negligible (fig. 17).

[b] C_1 = 1.01 pF, C_2 = 1107 pF, R_1 = 50 Ω, L_9 = 1 nH.
All other components are negligible (fig. 17).

Freq. (Hz)	V_o/V_{in}[c]	V_o/V_{in}[d]
6.0E + 1	8.865E – 5	8.865E – 5
6.0E + 2	9.113E – 5	9.113E – 5
6.0E + 3	9.115E – 5	9.115E – 5
6.0E + 4	9.115E – 5	9.115E – 5
6.0E + 5	9.115E – 5	9.102E – 5
6.0E + 6	9.115E – 5	9.101E – 5
6.0E + 7	9.115E – 5	7.682E – 5
6.0E + 8	9.115E – 5	1.363E – 3

[c] C_1 = 1.01 pF, C_2 = 1107 pF, R_1 = 9 $M\Omega$, R_2 = 1 $M\Omega$.
All other components are negligible (fig. 17).

[d] C_1 = 1.01 pF, C_2 = 1107 pF, R_1 = 9 $M\Omega$, R_2 = 1 $M\Omega$, L_9 = 1 nH.
All other components are negligible (fig. 17).

7. SUMMARY

Three different capacitive probes intended for use in measuring transient signals in gas-insulated systems were investigated. In a system, these probes form a capacitor divider but differ from the conventional capacitor divider in that the high side capacitance does not exist as a discrete component. This complicates the process of characterizing the probe, since the value of the high side capacitance is determined by the geometrical relation between the probe and the high voltage electrode.

One probe was a near-field scale model similar to that found in BPA equipment; a second was based on designs used in pulse power measurements; while the third was configured for ease of use in existing equipment. The model sensor was found to have serious shortcomings. Inductance associated with the assembly resulted in sensor behavior significantly different from that predicted by a simple equivalent circuit for a capacitive divider. This behavior was evidenced by large oscillations in the output, and a high level output voltage. The sensor was found to be useless for transient measurements.

A second probe, the plug probe, was similar to those described in the literature which had been used in both gas and liquid insulated pulse power systems. This divider had electrical characteristics which agreed, to within the measurement capabilities employed, with those calculated by using an ideal model for a capacitive divider. There was no evidence of device oscillation below 1 GHz, and no indication of low side inductance.

A third sensor had a disk geometry, and could be installed directly in place of the existing BPA sensors. This disk sensor compared favorably with the plug sensor, but could not be evaluated as thoroughly because of geometrical constraints in the test facility. The design of this sensor was not optimized and all laboratory tests were made on a "brass board" system.

A characteristic of capacitive dividers is the RC decay associated with the step response of the system. For many passive systems, this restricts their usefulness to waveform durations of less than 1 μs. The time constant can be increased by orders of magnitude by using active electronics in the low side. This may be done by employing fast buffer amplifiers (cable drivers) or commercial FET input probes. When this is done, there is some loss of rise time and decrease in reliability. For gas-insulated systems, the rise times achieved may be adequate, if primary interest is in observing waveforms which extend over the several hundred kHz to MHz range. If specific information about the rise time of the primary breakdown process is desired, then a passive probe can be used since long-term waveforms are not of interest.

The application of discrete component equivalent circuits was useful in understanding sensor behavior. These models provided upper limits to various stray inductances associated with the plug sensor. This knowledge is important in considering how to calibrate the sensor, since the low side impedance must be thoroughly characterized in the laboratory.

The problem of divider calibration remains largely unsolved. Calculations based on discrete component equivalent circuits show very small inductances in divider low sides can cause significant deviations from low frequency ratios at near GHz frequencies. Experimental and theoretical work was done using the approach of determining in the laboratory all relevant information about the divider except C_1. In principle, the magnitude of the voltage pulse propagating in the transmission line test facility can be calculated, but because of uncertainties in reflection coefficients at impedance mismatches, there is uncertainty in this procedure. A more accurate calculation would involve use of a well-characterized line, as determined by use of time domain reflectometry and a transient code such as EMTP. This approach was not explored in any detail, but does not involve any extension of existing technology. Since C_1 and C_2 can be accurately determined in the laboratory, a method exists for comparing experiment and theory.

The results of calculations of the steady-state response of the capacitive sensors over a wide frequency range demonstrate the futility of trying to do a calibration at 60 Hz unless inductance in the system can be kept well below 1 nH. The usefulness of this approach using active low side electronics was only explored in a preliminary way, and would require extensive effort for a comprehensive evaluation.

The experimental line as it presently exists is far from optimum. The facility would be much more useful if the impedance mismatches could be reduced to provide a more uniform impedance. In the high voltage mode, a cable extension to the line could provide a high voltage square wave with a duration of more than one microsecond without significant droop. The impedance of the overall line should be determined by using reflectometry methods to provide data necessary for computer modelling of pulse propagation on the line.

Since useful sensor designs have been determined, there should be emphasis placed on developing calibration methods for both laboratory and field application. This will require experimental and theoretical effort.

The usefulness of active electronics in the low side of the sensor has not been thoroughly investigated. Although this approach does extend the low frequency response of the system, the overall system capability has not been looked at. Information regarding system stability, thermal response and reliability is lacking.

Although the individual components of a measurement system consisting of sensor, low side electronics and optical links can be studied separately, it is advisable to determine the integrated system package response to signals of the type encountered in the field. The laboratory setting is an ideal setting in which to do this.

8. ACKNOWLEDGMENTS

9. REFERENCES

[1] Workshop on User Experience With Gas Insulated Substations, EPRI report
     EL-2189, Dec. 1981.

[2] Bibliography of Gas Insulated Substations, prepared by the Working Group
     on Gas Insulated Substations, paper 82WM169-1, IEEE PES Winter Meeting,
     Jan. 31-Feb. 5, 1982.

[3] S. Narimatsu, K. Yamaguchi, S. Nakano, and S. Maruyama, Interrupting
     Performance of Capacitive Current by Disconnecting Switch for Gas Insulated
     Switchgear, IEEE Trans. PAS 100, pp. 2726-2732, 1981.

[4] S. A. Boggs, F. Y. Chu, N. Fukimoto, A. Krenicky, A. Plessl, and D. Schlicht,
     Disconnect Switch Induced Transients and Trapped Charge in Gas Insulated
     Substations, paper 82WM003-2, IEEE PES Winter Meeting, Jan. 31-Feb. 5, 1982.

[5] L. Blahous and T. Gysel, Mathematical Investigation of the Transient
     Overvoltages During Disconnector Switching in GIS, paper 83WM109-6,
     IEEE PES Winter Meeting, Jan. 30-Feb. 4, 1983.

[6] N. Fujimoto, E. P. Dick, S. A. Boggs, and G. L. Ford, Transient Ground
     Potential Rise in Gas Insulated Substations - Experimental Studies,
     paper 82WM011-5, IEEE PES Winter Meeting, Jan. 31-Feb. 5, 1982.

[7] W. Pfeiffer, Ultra-High-Speed Methods of Measurement for the Investigation
     of Breakdown Development in Gases, IEEE Trans. Dist. and Meas., IM. 26,
     pp. 367-372, 1977.

[8] S. A. Boggs, G. L. Ford, and R. C. Madge, Coupling Devices for the
     Detection of Partial Discharges in Gas Insulated Switchgear, IEEE Trans.
     PAS-100, pp. 3969-3973, 1981.

[9] IRR-IMS Group, "Facing UHV Measuring Problems," Electra, No. 35,
     pp. 157-254, July 1974.

[10] K. Tokoro, Y. Harumoto, H. Yamamoto, Y. Yoshida, H. Mukae, Y. Ohno,
     M. Shimada, and Y. Ida, Development of Electronic Potential and Current
     Transducers Suitable for Gas Insulated Switchgear and Adequate for
     Application to Substation Digital Control System, paper 82WM172-5,
     IEEE PES Winter Meeting, Jan. 31-Feb. 5, 1982.

[11] D. Pellinen and M. S. D. Capua, Two-Megavolt Divider for Pulsed High
     Voltages in Vacuum, Rev. Sci. Inst. 51, pp. 70-73, 1980.

[12] D. F. McDonald, C. J. Benning, and S. J. Brient, Subnanosecond Rise Time
     Multikilovolt Pulse Generator, Rev. Sci. Inst. 36, pp. 504-506, 1965.

[13] G. E. Leavitt, J. D. Shipman, Jr., and I. M. Vitkovitsky, Ultrafast
     High Voltage Probe, Rev. Sci. Inst. 36, pp. 1371-72, 1965.

[14] A. J. Schwab and J. H. W. Pagel, Precision Capacitive Voltage Divider
     for Impulse Voltage Measurements, IEEE Trans. PAS 91, pp. 2376-2382, 1972.

[15] E. Kuffel and M. Abdullah, High Voltage Engineering, Pergamon Press, 1970.

[16] A. J. Schwab, High-Voltage Measurement Techniques, M.I.T. Press, 1972.

[17] A. Courts, BPA, private communication.

[18] N. W. Harris, High Voltage Probe for Liquid Imersion in Measurement of Electrical Quantities in Pulse Power Systems, R. H. McKnight and R. E. Hebner, eds., NBS Special Publication 628, pp. 20-25, 1982.

[19] M. Wilkinson and E. Chu, Calibration of Capacitive Voltage Probes in Water-Dielectric, High-Power Pulse Generators in Measurement of Electrical Quantities in Pulse Power Systems, R. H. McKnight and R. E. Hebner, eds., NBS Special Publication 628, pp. 59-68, 1982.

[20] N. Fijimoto, S. A. Boggs, and R. C. Madge, Measurement of Transient Potentials in Coaxial Transmission Lines Using Coaxial Dividers in Measurement of Electrical Quantities in Pulse Power Systems, R. H. McKnight and R. E. Hebner, eds., NBS Special Publication 628, pp. 69-79, 1982.

[21] E. Nolting, R. Martin, and M. Ruppalt, Electrical Measurement Techniques Used at the Casino Facility in Measurement of Electrical Quantities in Pulse Power Systems, R. H. McKnight and R. E. Hebner, eds., NBS Special Publication 628, pp. 118-132, 1982.

[22] G. P. Metzger, M. Riedinger, F. M. Schmitt, and G. L. Sutter, Measurement of Nanosecond Very High Voltage Pulses, Nucl. Inst. Methods, 61, pp. 226-228, 1968.

[23] W. A. Edson and G. N. Oetzel, Capacitance Voltage Divider for High-Voltage Pulse Measurement, Rev. Sci. Inst., 52, pp. 604-606, 1981.

[24] C. A. Ekdahl, Voltage and Current Sensors for a High-Density Z-Pinch Experiment, Rev. Sci. Inst., 51, pp. 1645-1651, 1980.

[25] T. Haroda, Y. Aoshuma, M. Harada, and K. Huva, Development of High-Performance Low Voltage Arms for Capacitive Voltage Divider, paper 42.14 presented at the Third International Symposium on High Voltage Engineering, Milan, August 28-32, 1979.

[26] C. Trivelpiece, R. Richardson, J. Shaumer, and J. B. Smith, Digital Correction of Cable Attenuation Losses, in Measurement of Electrical Quantities in Pulse Power Systems, R. H. McKnight and R. E. Hebner, eds., NBS Special Publication 628, pp. 381-391, 1982.

[27] An application of a fast buffer amplifier was described by Dr. W. J. Sargeant in Measurment of Electrical Quantities in Pulse Power Systems, R. H. McKnight and R. E. Hebner, eds., NBS Special Publication 628, pp. 170-173, 1982.

4. TITLE AND SUBTITLE

EVALUATION OF TRANSIENT MEASUREMENT METHODS
IN GAS-INSULATED TRANSMISSION LINES

5. AUTHOR(S)

Ronald H. McKnight and Howard K. Schoenwetter

6. PERFORMING ORGANIZATION (If joint or other than NBS, see instructions)

NATIONAL BUREAU OF STANDARDS
DEPARTMENT OF COMMERCE
WASHINGTON, D.C. 20234

7. Contract/Grant No.

8. Type of Report & Period Covered

11. ABSTRACT (A 200-word or less factual summary of most significant information. If document includes a significant bibliography or literature survey, mention it here)

Capacitive sensors suitable for measuring transients in gas-insulated transmission lines have been studied in the laboratory. Measurements of the step response of three different sensors were made with a test line using both low voltage (200 V) and high voltage (10 kV) signals. Sensor designs were based on those used in pulse power measurements. The use of active electronics at the sensor output in the form of fast buffer amplifiers or commercial FET input probes was investigated as a means of extending low frequency cutoff. Lumped parameter models were used to provide theoretical analysis of experimental results.

12. KEY WORDS (Six to twelve entries; alphabetical order; capitalize only proper names; and separate key words by semicolons)

capacitor sensors; gas-insulated equipment; high voltage;
transient measurements; transmission lines.